nature communications

Article

https://doi.org/10.1038/s41467-026-70124-9

Alpha frequency shapes perceptual sensitivity by modulating optimal phase likelihood

Received: 8 March 2024

Accepted: 13 February 2026

Published online: 03 March 2026

Check for updates

Vincenzo Romei [1,2,3] & Luca Tarasi [1,3]

Whether alpha frequency oscillations orchestrate the pace of sensory sampling is current matter of debate. Using EEG, we test this hypothesis by investigating whether pre-stimulus instantaneous alpha frequency accounts for perceptual sensitivity. Our results support the role of alpha frequency in shaping the accuracy of sensory acquisition. Spontaneous alpha frequency inter-trial fluctuations emerged as a predictor of perceptual decision-making sensitivity and accuracy, with higher pace accounting for higher sensory precision - an observation supported across complementary analytical approaches, including Bayesian statistics and computational modelling. Here, we provide insights into the neural candidate mechanisms through which alpha frequency relates to perceptual decisions. Specifically, alpha frequency would determine the extent of phase angles covered within the stimulus timeframe. As a result, higher alpha frequencies may provide more opportunities for the stimulus to coincide with optimal phases for perception, thereby increasing the likelihood of accurate sensory processing.

Converging evidence supports the concept that the human perceptual machinery functions as a discrete system[1] that samples the continuous stream of incoming sensory information into distinct integration windows[2]. Similar to other sampling-based processes, the acquisition rate plays a fundamental role in determining the accuracy and fidelity of the resultant representation. Specifically, higher sampling frequencies are associated with a more precise representation of the source signal. Alpha rhythms (7–13 Hz) have emerged as a prominent neurobiological candidate involved in governing the parsing of sensory processing into distinct units[3]. Consequently, we postulated that higher alpha oscillation frequencies may be connected to heightened perceptual resolution, thereby enhancing the sensitivity and fidelity of the visual experience[4,5]. This hypothesis is grounded on several studies[6–8], which demonstrated that both inter-individual and intra-individual differences in individual alpha frequency (IAF) during task performance play a significant role in explaining perceptual outcome and the temporal resolution of the visual system. For example, a higher pre-stimulus alpha frequency was predictive of higher accuracy in discriminating two flashes in the two-flash fusion (2FF) task[9,10] and individuals with a lower occipital IAF had elongated windows of illusion in a sound-induced flash illusion (SIFI) paradigm[11,12]. Additionally, we have recently demonstrated that individuals with a higher resting IAF require less contrast for accurate detection compared to low IAF participants[13]. Crucially, the reduction vs. acceleration of alpha frequency by means of neurostimulation enlarged vs. shrunk the sensory integration window, influencing susceptibility to experiencing the SIFI[11,14]. Furthermore, transcranial Alternating Current Stimulation (tACS) applied at different frequencies within the alpha band can alter participants' perceptual switching rate in a bistable colour-motion binding stimulus, where higher alpha frequencies resulted in accelerated perceptual switches by shortening perceptual epochs of active binding[15]. Recent studies[16,17] have further underscored that the direction of IAF modulations varies depending on whether a task requires sensory segregation or integration, with IAF tending to increase during segregation tasks and decrease during integration tasks.

[1]Dipartimento di Psicologia, Università di Bologna and Centro studi e ricerche in Neuroscienze Cognitive, Università di Bologna, Cesena, Italy. [2]Universidad Antonio de Nebrija, Madrid, Spain. [3]These authors contributed equally: Vincenzo Romei, Luca Tarasi. e-mail: vincenzo.romei@unibo.it; luca.tarasi2@unibo.it

Despite this recent converging evidence suggesting a role for alpha frequency in sensory sampling, a recent study by Buerges and Noppeney[18] deviated from the prevailing evidence in the field. Indeed, they found, in a sample of 20 individuals within the general population, that neither inter-individual differences nor inter-trial variations in IAF account for performance outcomes in both a 2FF task and a yes/no detection task. Furthermore, the authors highlighted that the link between IAF and perceptual performance found in previous studies could be undermined due to an unaddressed confounding factor associated with participants' response bias. In addition to the limitations pinpointed by Buerges and Noppeney, other unresolved issues can be identified in the previous literature findings. For example, most studies examining IAF-related effects on behaviour employed small sample sizes, which is especially concerning according to a recent meta-analysis suggesting a minimum of 50 participants necessary to detect robust effects[6]. Furthermore, the majority of previous studies investigating this scientific question used the traditional trial-averaging technique. Consequently, there is a lack of robust approaches that enable the exploration of the finer trial-by-trial relationship between IAF fluctuations and behavioural outcomes. Additionally, the existing body of evidence has primarily investigated a potential role for IAF in modulating perceptual temporal resolution rather than delving into its direct impact on shaping sensory accuracy (but see refs. 13,19). Here, we posit that alpha rhythm may serve as a general neural code underpinning perceptual sampling, influencing both temporal and perceptual resolution. The underlying process can be understood through the classic 2-flash fusion task. In this task, authors have proposed that when two flashes of light are presented within the same alpha cycle, they are perceived as a single flash because they are integrated within the same temporal window. Conversely, when the flashes fall in different alpha cycles, they are perceived as two distinct events, due to separate sampling moments[9,11]. Building on this concept, we hypothesise that the same mechanism governs the relationship between IAF and perceptual resolution. For example, if a visual stimulus is presented in a way that it spans across two different alpha cycles, it will be sampled twice by the brain, leading to a clearer and more distinct perception. However, if the stimulus falls within a single alpha cycle, it is processed only once, potentially reducing perceptual performance.

In addition, existing evidence has not investigated the specific mechanism linking higher IAF to more faithful representations of reality. Here we test the hypothesis that higher vs. lower IAF allows for higher probability of optimal alpha phase to catch even short-lasting stimuli, leading to successful sensory processing. Specifically, the hypothesis is based on compelling evidence showing that the accuracy of decision-making relies on the precise phase of alpha waves during the peri-stimulus period[20–22]. The basic idea we propose here is that the mechanism facilitating a more accurate response with higher (relative to lower) IAF lies in its capacity to span a broader distribution of phase angles within the same stimulus presentation timeframe. As a consequence, this heightened phase coverage increases the likelihood of aligning with optimal phase angles, crucial for the accurate perception of stimuli. This proposition, in turn, leads to another hypothesis closely intertwined: the ability of phase angles in dictating the accuracy of the response is expected to be more pronounced in participants or trials in which IAF is lower. In such instances, the reduced likelihood of falling into optimal phases during stimulus processing makes the phase angles an important determinant of performance (i.e. if the phase is in non-optimal angles, the likelihood of reaching the optimal ones will be reduced). On the contrary, when alpha is higher, it aids in covering numerous phase angles during stimulus presentation, thereby increasing the likelihood of processing stimuli within those optimal phases. Our experimental design was particularly suited to capture this relationship given the presentation time of our stimuli (i.e. 59 ms), where the phase position becomes more critical due to the limited time available to cover a wide distribution of phase angles.

In this work, we examine how pre-stimulus instantaneous alpha frequency relates to perceptual sensitivity during visual detection in a contrast detection paradigm. Using EEG, we recorded brain activity non-invasively from participants while they reported the presence of grey circles embedded in black and white checkerboard patterns. Each checkerboard was presented for 59 ms and the contrast of the grey circles was titrated for each individual to their 70% perceptual accuracy. To test for the role of IAF as a candidate sampling mechanism, we have undertaken a multi-faceted approach. First, we have employed a big-data approach, analysing our hypothesis in a large sample ($n = 125$) of individuals within the general population. Secondly, we supplemented the frequentist analyses with Bayesian statistics (Bayes Factor) to provide an estimate of the effect's strength and direction. Third, we have exploited computational models such as the signal detection theory (SDT) framework to disentangle potential IAF effects related to sensitivity vs. bias. Fourth, we analysed a potential relationship between IAF and decisional parameters extracted using the drift diffusion model (DDM), the most commonly used computational framework for modelling human perceptual decision-making[23–25]. Fifth, we have complemented classic binning methods with more robust analyses that evaluated the trial-by-trial relationship between IAF and behaviour[26]. Subsequently, we delineated a candidate mechanism enabling a higher IAF to process stimuli more faithfully, demonstrating the inherent interplay between alpha frequency and phase. To this end, we employed both bin-based and trial-by-trial analyses using alpha phase, IAF and their interaction as predictors. We find that moment-to-moment variations in alpha frequency are associated with differences in accuracy and sensitivity. We also observe that alpha phase relates to perceptual accuracy, and that this phase–accuracy relationship depends on the prevailing alpha frequency. Finally, we outline a candidate framework in which higher alpha frequency increases the number of phase angles sampled during stimulus presentation, thereby increasing the chance that the stimulus coincides with phases more favourable for perception.

Results

We assessed the influence of alpha frequency and alpha phase in dictating the accuracy of perceptual reporting in a visual detection paradigm. Using EEG, we recorded brain activity non-invasively from 125 participants while they reported the presence of grey circles embedded in black and white checkerboard patterns (Fig. 1).

Each checkerboard was presented for 59 ms and the contrast of the grey circles was titrated for each individual to their 70% perceptual accuracy. In half of the trials, checkerboards did not contain any grey circle embedded in them (catch trials). Participants were instructed to indicate via the keyboard the presence (key 'k') or absence (key 'm') of the grey circles inside the checkerboard. No timeout was set for the response. After collecting the response, the screen appeared black for 1.9–2.4 s in the inter-trial interval. On average, participants reached 73.5 % accuracy, testifying to the accuracy of the titration procedure employed. The average RT for the task was 0.88 ± 0.03 s. Correct responses had faster RT (0.85 ± 0.03 s) compared to the slower RT for incorrect responses (0.99 ± 0.04 s; see Fig. 1B).

We investigated whether fluctuations in prestimulus alpha frequency, alpha phase and their interaction were linked to perceptual decision-making. To this end, first we computed the first temporal derivative of the phase angle time series (see 'Methods'), representing the instantaneous frequency of a signal within a band-limited range[27]. We focused our analysis on a pool of occipito-parietal electrodes located on the midline and right side (i.e. Oz, POz, O2, PO4, PO8), selecting, for each subject, the electrode that exhibited the maximum alpha power in the prestimulus window. These electrodes were chosen

https://doi.org/10.1038/s41467-026-70124-9

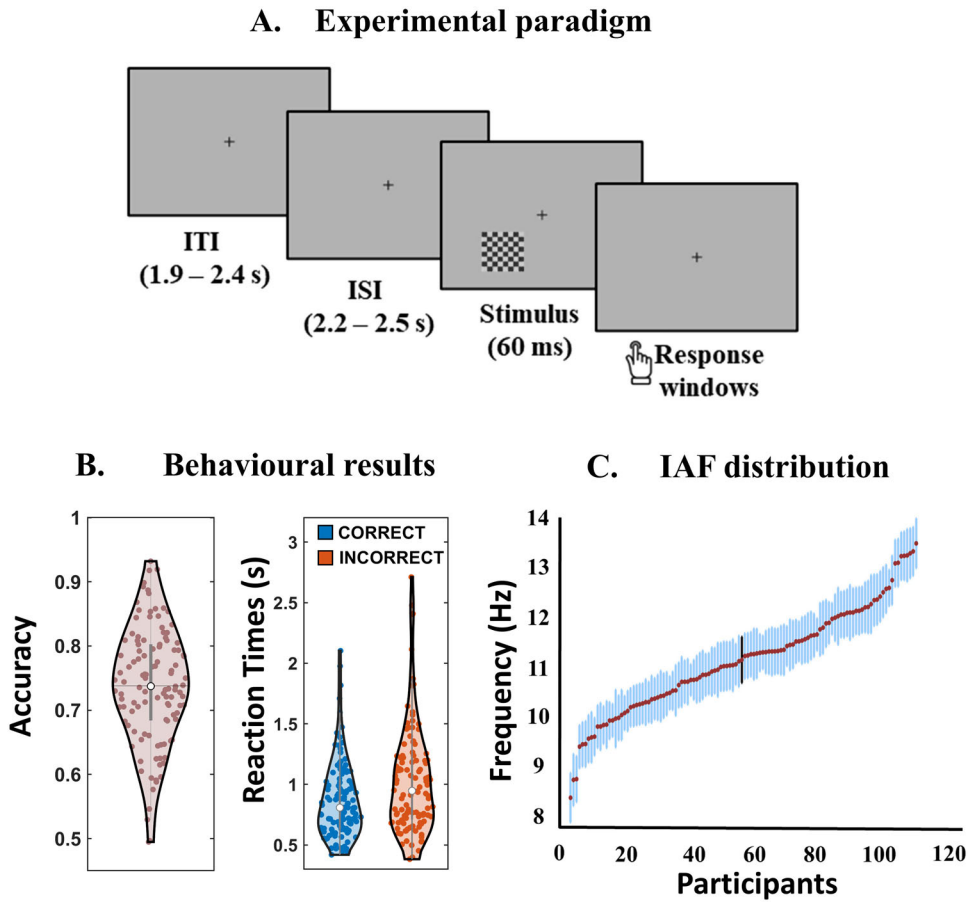

Fig. 1 | Experimental design and individual alpha frequency (IAF) distribution. **A** Schematic representation of the task. Stimuli were presented on an 18" CRT display at ~57 cm in a dimly lit room. Participants indicated the presence (key 'k') or absence (key 'm') of grey circles within checkerboards in the lower left visual field. After a titration phase to determine the contrast level for 70% detection accuracy, each trial began with a neutral cue for 1 s, followed by a fixation dot and then the checkerboard stimulus for 59 ms. The inter-trial interval lasted between 1.9 and 2.4 s. **B** Behavioural results of the task. Participants ($n = 116$) achieved 73.5 ± 0.84% (Mean ± SE) accuracy (25th percentile = 68.48%, 75th percentile = 80.23%). The average reaction time (RT) for the task was 0.88 ± 0.03 s (Mean ± SE). Correct responses had a faster RT ($M = 0.85$ s, SE = 0.03 s, 25th percentile = 0.63 s, 75th percentile = 1.03 s), while incorrect responses were slower ($M = 0.99$ s, SE = 0.04 s, 25th percentile = 0.72 s, 75th percentile = 1.22 s). **C** Distribution of Individual Alpha Frequency (IAF) across sample ($N = 116$). The panel shows each participant's mean IAF value (dots), accompanied by their within-subject SEM (vertical bars), illustrating both between-participant and within-participant variability in alpha frequency. The mean IAF was 11.34 Hz (25th percentile = 10.57 Hz, 75th percentile = 11.98 Hz), with a standard deviation of 0.89 Hz across time, trials and participants, highlighting the variability in alpha frequency within the sample. The Shapiro-Wilk test indicated that IAF follows a normal distribution ($p = 0.429$). A two-sided Pearson correlation further revealed a positive relationship between IAF and variability, with higher IAF values being associated with greater variability ($r = 0.37$, $p < 0.001$).

because the stimulus was consistently presented on the left. Then, we evaluated, using a diverse range of statistical methods, whether there was an effect of IAF on perceptual outcome. Secondly, we assessed whether phase angles could distinguish between correct and incorrect decision and, finally, we evaluated any interaction between IAF and alpha phase able to shed light on the candidate mechanisms underlying their effect on sensory precision.

Pre-stimulus IAF is linked to variations in perceptual sensitivity

We investigated the influence of pre-stimulus IAF on perceptual sensitivity and bias by employing a binning analysis. This analysis involved dividing the trials into three terciles based on pre-stimulus IAF[18]. We time-collapsed the IAF data by computing the average values from −800 ms to −100 ms for each participant. First, we showed strong evidence (BF = 59.79) for a difference in accuracy between the third IAF tercile (mean accuracy = 0.76, SE = 0.01) compared to the first IAF tercile (mean accuracy = 0.72, SE = 0.01; $t_{115} = -3.71$, $p < 0.001$; Fig. 2A). Subsequently, we computed the signal detection indices from trials within the first and third terciles. The results demonstrated that trials in the first tercile were associated with reduced sensitivity (mean d' = 1.46, SE = 0.07) compared to trials within the third tercile (mean d' = 1.65, SE = 0.07; $t_{115} = -3.10$, $p = 0.003$; Fig. 2B), indicating moderate evidence for a difference (BF = 9.32). Conversely, the criterion indices estimated in the first (mean c = 0.44, SE = 0.04) vs. third terciles (mean $c = 0.39$, SE = 0.04) were not statistically different ($t_{115} = 1.67$, $p = 0.098$, Fig. 2C), providing anecdotal evidence (BF = 0.39). This finding suggests that trials with higher IAF are associated with higher perceptual sensitivity and accuracy, while the response bias does not appear to be predicted by IAF. The pattern of results remained consistent when using two or four IAF bins (See Supplementary Method 1). Furthermore, we found no statistical differences in behavioural performance when binning trials based on pre-stimulus power (Fig. S2). Moreover, building on our recent finding that individuals with higher resting IAF require less contrast for accurate detection compared to those with lower IAF[13], we further demonstrate that this relationship extends to average pre-stimulus alpha levels. Specifically, individuals with higher pre-stimulus IAF consistently required lower threshold contrast to achieve target performance levels (Pearson = −0.21, $p = 0.021$; Pearson skipped = −0.21, CI = [−0.37, −0.03]), although the BF indicated only limited evidence for this association (BF = 1.04).

https://doi.org/10.1038/s41467-026-70124-9

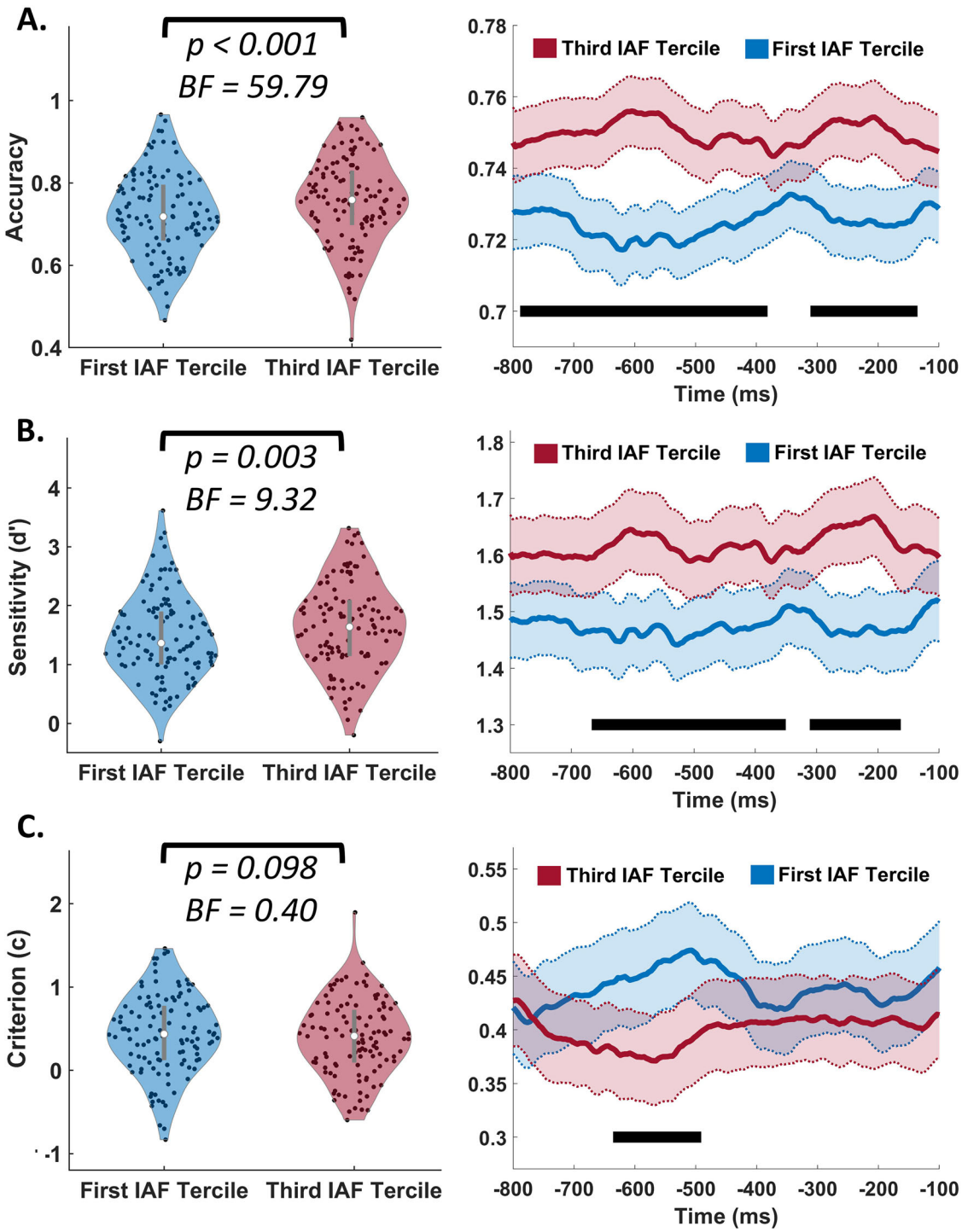

Fig. 2 | Binning analysis on IAF. A The left panel shows that detection accuracy across sample ($N = 116$) was higher in trials belonging to the third IAF tercile ($M = 0.76$, SE = 0.01; 25th percentile = 0.70; 75th percentile = 0.83) compared to the first tercile ($M = 0.72$, SE = 0.01; 25th percentile = 0.66; 75th percentile = 0.79), as assessed by a two-sided paired t-test ($t_{115} = -3.71$, $p < 0.001$). The right panel shows the time-resolved analysis performed using a two-sided cluster-based permutation test (1000 permutations; cluster-corrected), which revealed two significant clusters where accuracy was higher for high-IAF trials (−800 to −390 ms, cluster $p < 0.001$; −310 to −135 ms, cluster $p = 0.009$). **B** The left panel shows that sensitivity was higher in the third ($M = 1.65$, SE = 0.07; 25th percentile = 1.15; 75th percentile = 2.09) than in the first ($M = 1.46$, SE = 0.07; 25th percentile = 1.01; 75th percentile = 1.89) IAF tercile, as assessed with a two-sided paired t-test ($t_{115} = -3.10$, $p = 0.003$). The right panel shows the two-sided cluster-based permutation test, which identified two significant intervals where sensitivity was higher in high-IAF trials (−670 to −350 ms, cluster $p < 0.001$; −310 to −160 ms, cluster $p = 0.015$). **C** The left panel shows no significant difference in criterion between the first ($M = 0.44$, SE = 0.04) and third ($M = 0.39$, SE = 0.04) IAF terciles, as tested with a two-sided paired t-test ($t_{115} = 1.67$, $p = 0.098$). The right panel shows a two-sided cluster-based permutation test, which identified a significant cluster (−635 to −490 ms, cluster $p = 0.036$) indicating reduced decisional bias (criterion closer to 0) in high-IAF trials. Significant time points are indicated with black lines ($p < 0.05$; permutation test; cluster corrected). Shaded regions denote mean ± within-subjects SE.

Time-resolved binning analysis revealed that the IAF effect on sensitivity is broadly extended over the pre-stimulus period

Having examined the impact of pre-stimulus IAF on perceptual sensitivity using a binning approach, we then extended our analysis to explore the time dynamics of the effect similar to[18]. For this purpose, we re-sorted the trials into three bins based on the prestimulus instantaneous frequency. However, this time the procedure was iterated for each pre-stimulus time point separately. Subsequently, we entered sensitivity (d'), criterion (c) and accuracy indices extracted in each time point into a cluster-based statistic to examine the time-resolved nature of the effect (See 'Methods'). The results indicated that, both accuracy (Fig. 2A) and sensitivity (Fig. 2B), demonstrated statistically significant differences between the types of trials, further corroborating the findings highlighted in the previously conducted time-averaged analysis. Specifically, accuracy was higher in the third than in first IAF terciles within two temporal clusters: one ranging from −800 ms to −390 ms (p cluster < 0.001) and another from −310 ms to −135 ms (p cluster = 0.009). Furthermore, we observed increased d' in the third IAF tercile compared to the first IAF tercile in the time period ranging from −670 ms to −350 ms ($p < 0.001$) and in the period ranging from −310 ms to −160 ms ($p = 0.015$). Similarly, when extending the analysis to a broader prestimulus window (−2500 to −100 ms), we found that IAF predicted sensitivity and accuracy already ~1.5 s before stimulus onset (Fig. S1). However, these long-range effects became stronger and more consistent within the immediate prestimulus interval selected for the main analysis (−800 to −100 ms). Finally, this time-resolved analysis revealed an effect on the criterion that was not evident when averaging values across the temporal dimension (Fig. 2C). Specifically, in the interval from −635 to −490 ms ($p = 0.036$), there was a reduction in decisional bias, as indicated by the criterion moving closer to the 0 value, in trials characterised by higher IAF compared to those with lower IAF. This suggests that more accurate sampling of the external signal may have indirectly contributed to a reduction in perceptual bias. This is confirmed by a negative association between perceptual accuracy and bias, with higher sensitivity associated with lower bias (Pearson = −0.299, $p = 0.001$; BF = 15.02; Pearson skipped = −0.24, CI = [−0.39; −0.06]).

IAF is higher in correct vs. incorrect trials

Finally, we explored whether the frequency of alpha oscillations before stimulus presentation could also shed light on the distinction between correct and erroneous responses. Thus, we compared IAF preceding correct vs incorrect response. The analysis (Fig. 3A) yielded a significant effect ($t_{115} = 4.13$, $p < 0.001$), indicating very strong evidence for a difference (BF = 245.51). Specifically, higher alpha frequency was associated with a correct response ($M = 11.35$ Hz, SE = 0.1 Hz, 25th percentile = 10.60, 75th percentile = 11.97), while lower alpha frequency was linked to a higher chance of errors ($M = 11.30$ Hz, SE = 0.10 Hz, 25th percentile = 10.61, 75th percentile = 11.97). Moreover, we showed (see Supplementary Method 2) that IAF does not significantly predict the actual choice (i.e. reporting 'present' vs. 'absent'). In addition, we demonstrated that there is no statistical relationship between detection accuracy and alpha power, as alpha power does not differ between correct and incorrect trials (Fig. S3).

Trial-by-trial fluctuations in IAF predict the accuracy of perceptual report

The statistical methods presented so far go in line with the traditional cognitive electrophysiology analyses that rely on data averaging over trials to maximise the signal-to-noise ratio. In recent times, there has been a growing trend among researchers to employ single-trial analyses to link EEG activity with metrics of interest defined at the single-trial level. This approach enables the exploration of the trial-by-trial relationship between brain activity and behaviour/perception, which is not observable when using traditional averaging-based methods. To this end, we employed a multiple regression approach using a least-squares solution[28] to examine a link between single-trial estimates of IAF and single-trial accuracy. The conducted analysis demonstrated a positive association between trial-by-trial variations in IAF and perceptual accuracy ($t_{115} = 4.42$, $p < 0.001$; Fig. 3B). This finding implies that trials in which IAF was higher vs. lower were associated with accurate responses (mean slope = 0.43, SE = 0.10). A Bayesian paired t-test yielded BF = 708.91, providing very strong evidence for this association. Crucially, we ruled out the hypothesis that the relationship between IAF and perceptual sensitivity is merely due to spurious changes in alpha frequency reflecting variations in the power of different alpha generators. Our source analysis demonstrates that all the observed effects are predicted by the IAF extracted from occipital sources, further confirming the specific role of occipital areas in accounting for sensory precision[29,30] (See Supplementary Method 3). While our source-level reconstruction corroborated the sensor-space findings, the intrinsic limitations of EEG spatial resolution and potential source mixing constrain the anatomical specificity of these effects.

Moreover, we found no statistical relationship between IAF and RT on a trial-by-trial basis (Supplementary Method 4, mean slope = 0.05, SE = 0.10, $t_{115} = 0.52$, $p = 0.603$), providing strong evidence for the absence of an association (BF = 0.12). This demonstrates that the impact of IAF on accuracy is unlikely to reflect a speed/accuracy trade-off. If such trade-off were present, higher IAF would be expected to correlate with slower reaction times, as individuals might prioritise accuracy over speed; however, the strong evidence for no association between IAF and RT supports the interpretation that IAF directly enhances response accuracy without affecting response speed. Finally, no statistical relationship was observed between fluctuations in alpha power and perceptual sensitivity (See Fig. S4).

Trial-by-trial fluctuations in IAF predict the accuracy of sensory accumulation

We expanded the previous trial-by-trial analysis, analysing the impact that IAF fluctuations had on DDM parameters. Unlike SDT, the DDM allows for simultaneous consideration of choice accuracy and full response time distributions, enabling a better tracing of decision dynamics. From the fitted DDM model, we extracted the drift rate (v), representing the rate of evidence accumulation, the starting point (z), capturing response bias, the boundary separation (a), indicating the amount of information required to decide and the non-decisional time (t), accounting for the time taken for processes other than perceptual decision-making. Using regression coefficients, we examined the relationship between trial-to-trial variations in IAF and the DDM parameters. Our analysis revealed a significant positive association between increased IAF and drift rate parameters (posterior mean IAF ~v coefficient = 0.049, HDI = [0.026; 0.073], Fig. 3C; $q < 0.001$). This finding indicates that in trials with relatively higher IAF sensory information are accumulated in a faster and more precise fashion. Interestingly, we found that IAF was unrelated to the starting point and the non-decisional time parameter (posterior mean IAF ~z coefficient = 0.001, HDI = [−0.003; 0.005], posterior mean IAF ~t coefficient = −0.001, HDI = [−0.004; 0.002], all $q > 0.34$), while there was an association with the boundary separation (posterior mean IAF ~a coefficient = 0.013, HDI = [−0.001; 0.026], $q = 0.031$), indicating that in trials with lower IAF there was a tendency to accumulate less information before deciding. These results provide valuable insights into the relationship between pre-stimulus IAF and the dynamic process of evidence accumulation during decision-making.

Instantaneous alpha phase shapes perceptual accuracy

In order to investigate the potential role of IAF phase in explaining the relationship between IAF and perceptual accuracy, we first investigated whether alpha phase could have an impact on perceptual accuracy by employing a binning analysis. Therefore, we grouped trials

https://doi.org/10.1038/s41467-026-70124-9

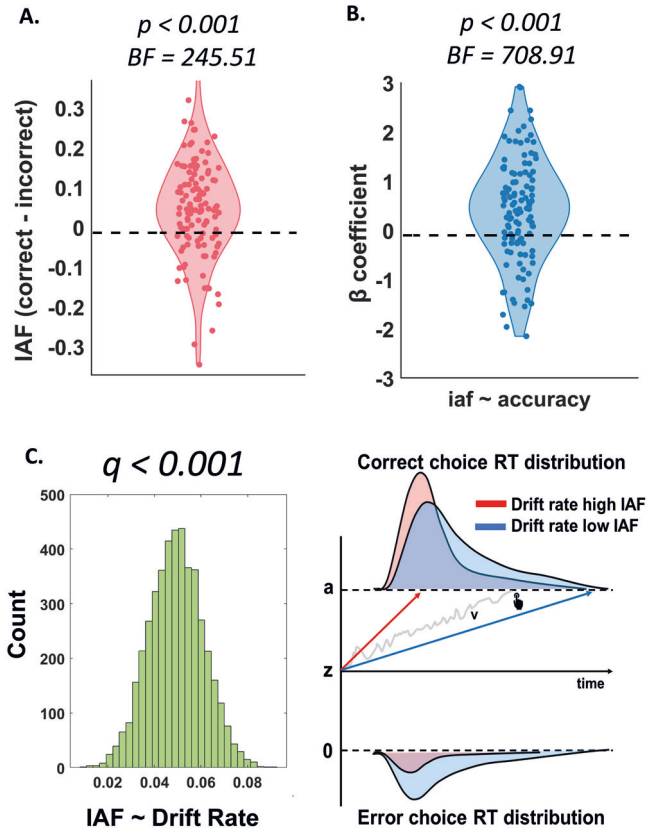

Fig. 3 | Trial-by-trial fluctuations of IAF shape sensory precision. A Alpha frequency unfolded at a relatively faster pace before accurate trials compared with erroneous ones [Δ IAF (Correct–Incorrect): $M = 0.05$ Hz, SE = 0.01 Hz, 25th percentile = −0.02 Hz, 75th percentile = 0.13 Hz]. This effect was assessed using a two-sided paired *t*-test ($t_{115} = 4.13$, $p < 0.001$), with the Bayes factor providing very strong evidence for a difference (BF = 245.51). Higher alpha frequency was associated with correct responses ($M = 11.35$ Hz, SE = 0.10 Hz, 25th percentile = 10.60, 75th percentile = 11.97), whereas lower alpha frequency preceded errors ($M = 11.30$ Hz, SE = 0.10 Hz, 25th percentile = 10.61, 75th percentile = 11.97). **B** The single-trial regression of accuracy on IAF showed that prestimulus alpha frequency prior to target onset was positively associated with detection accuracy. Trial-by-trial fluctuations in IAF reliably predicted perceptual accuracy (one-sample *t*-test, two-tails, $t_{115} = 4.42$, $p < 0.001$). Trials with higher relative IAF were more likely to yield accurate responses (mean slope = 0.43, SE = 0.10). A Bayesian paired *t*-test confirmed this effect (BF = 708.91), providing very strong evidence for the association. **C** Traces of the posterior samples derived from the HDDM model. Single-trial regression analysis unveiled that spontaneous fluctuations in IAF before target onset were positively correlated with the drift rate parameter (posterior mean v coefficient = 0.049, HDI = [0.026; 0.073], $q < 0.001$). In addition, this correlation was observed without a similar association with the starting point parameter (posterior mean z coefficient = 0.001, HDI = [−0.003; 0.005], $q = 0.392$), testifying a null effect of IAF in shaping decisional bias.

of similar phase together into two bins separately for each participant and timepoints in the −800 ms to 200 ms window. Each phase bin comprised 180° phase. The first bin contained all trials with phases between 0° and 180°, while the second one all trials between 180° and 360°. Subsequently, we entered accuracy indices calculated in the two bins and extracted in each time point into a cluster-based statistic to investigate the presence of clustered time points in which phase bins impact accuracy. The results indicated that accuracy exhibited a statistically significant difference between the two bins [time period ranging from −49 ms to −21 ms ($p = 0.007$), from 5 ms to 25 ms ($p = 0.014$), from 52 ms to 71 ms ($p = 0.027$), from 99 ms to 130 ms ($p = 0.008$) and from 157 ms to 177 ms ($p = 0.046$), Fig. S6].

Alpha phase effects on perceptual sensitivity are moderated by IAF

Having demonstrated that stochastic fluctuations in alpha phase are able to shape perceptual accuracy, we investigated whether IAF could play a moderator role on this relationship. The logic underlying this choice is that an individual who exhibits a higher alpha frequency covers more phase angles in the same amount of time compared to an individual with a lower alpha frequency. Therefore, the positioning of the phase at specific time points should have a greater impact in explaining decision outcomes in individuals with lower (compared to higher) IAF, as they will less likely show a transition from the favourable to unfavourable bin at critical time points, i.e. during stimulus presentation. To investigate this hypothesis, we replicated the above-mentioned analysis separately in individuals that exhibited lower vs. higher pre-stimulus IAF. We found that, in lower prestimulus IAF individuals, the two phase bins were associated with different levels of accuracy [Fig. 4A; time periods ranging from −685 ms to −666 ms ($p = 0.048$), −639 ms to −619 ms ($p = 0.029$), −588 ms to −564 ms ($p = 0.030$), 5 ms to 17 ms ($p = 0.045$) and 52 ms to 67 ms ($p = 0.046$)]. In contrast, no statistically significant phase bin differences were observed in individuals showing higher prestimulus IAF (Fig. 4B). Indeed, in this group, no cluster emerged in which alpha phase was able to predict perceptual accuracy. A complementary within-subject, cluster-based permutation test on the interaction contrast confirmed that this difference reflects a genuine IAF × phase interaction. Specifically, the modulatory effect of alpha phase on accuracy was significantly stronger in trials with low instantaneous IAF compared to high IAF (Fig. S7).

Trial-by-trial fluctuations in alpha phase predict perceptual sensitivity only in lower IAF trials

In order to corroborate the previous results that assessed the impact of alpha phase in groups of individuals exhibiting low vs. high prestimulus alpha frequency, we conducted trial-by-trial analyses evaluating, across the entire sample, whether there was a significant interaction between IAF and alpha phase. This analysis further demonstrated a positive association between trial-by-trial variations in IAF and perceptual accuracy (mean slope = 0.42, SE = 0.09; $t_{115} = 4.42$, $p < 0.001$), providing very strong evidence for an association (BF = 705.60). Moreover, we found that alpha phase significantly and strongly (BF = 14.64) impacts perceptual accuracy (mean slope = 0.29, SE = 0.09; $t_{115} = 3.26$, $p = 0.002$). Crucially, we found the presence of a significant negative interaction term between IAF and alpha phase (mean slope = −0.20, SE = 0.09; $t_{115} = -2.28$, $p = 0.024$), although the corresponding BF indicates limited evidence for this effect (BF = 1.24). We replicate this pattern of results employing a DDM analysis that included IAF, alpha phase and the IAF*phase interaction as predictors (Fig. 4C). The analysis demonstrated that IAF (posterior mean IAF -v coefficient = 0.071, HDI = [0.037; 0.110], $q < 0.001$) and instantaneous alpha phase (posterior mean Alpha phase -v coefficient = 0.064, HDI = [0.017; 0.110], $q = 0.002$) significantly impacted the drift rate parameters. Again, we found a significant negative interaction between IAF and alpha phase (posterior mean Alpha phase* IAF -v coefficient = −0.041, HDI = [−0.087; 0.001], $q = 0.043$). Crucially, none of these predictors, nor their interactions, significantly impacted the other DDM parameters (all $q > 0.072$), except for a significant relationship between alpha phase and the starting point parameter (posterior mean Alpha phase -z coefficient = 0.009, HDI = [0.001; 0.017], $q = 0.019$), where peak values were associated with a more neutral bias. This finding pointed to a reduced vs. increased influence of alpha phase in dictating perceptual sensitivity when the prestimulus alpha was higher vs. lower.

Correct vs. incorrect decisions are associated with a different phase angle only in the low IAF group

To further validate our findings beyond the bin-based approach on phase angles, we employed a reverse data-driven method to examine

https://doi.org/10.1038/s41467-026-70124-9

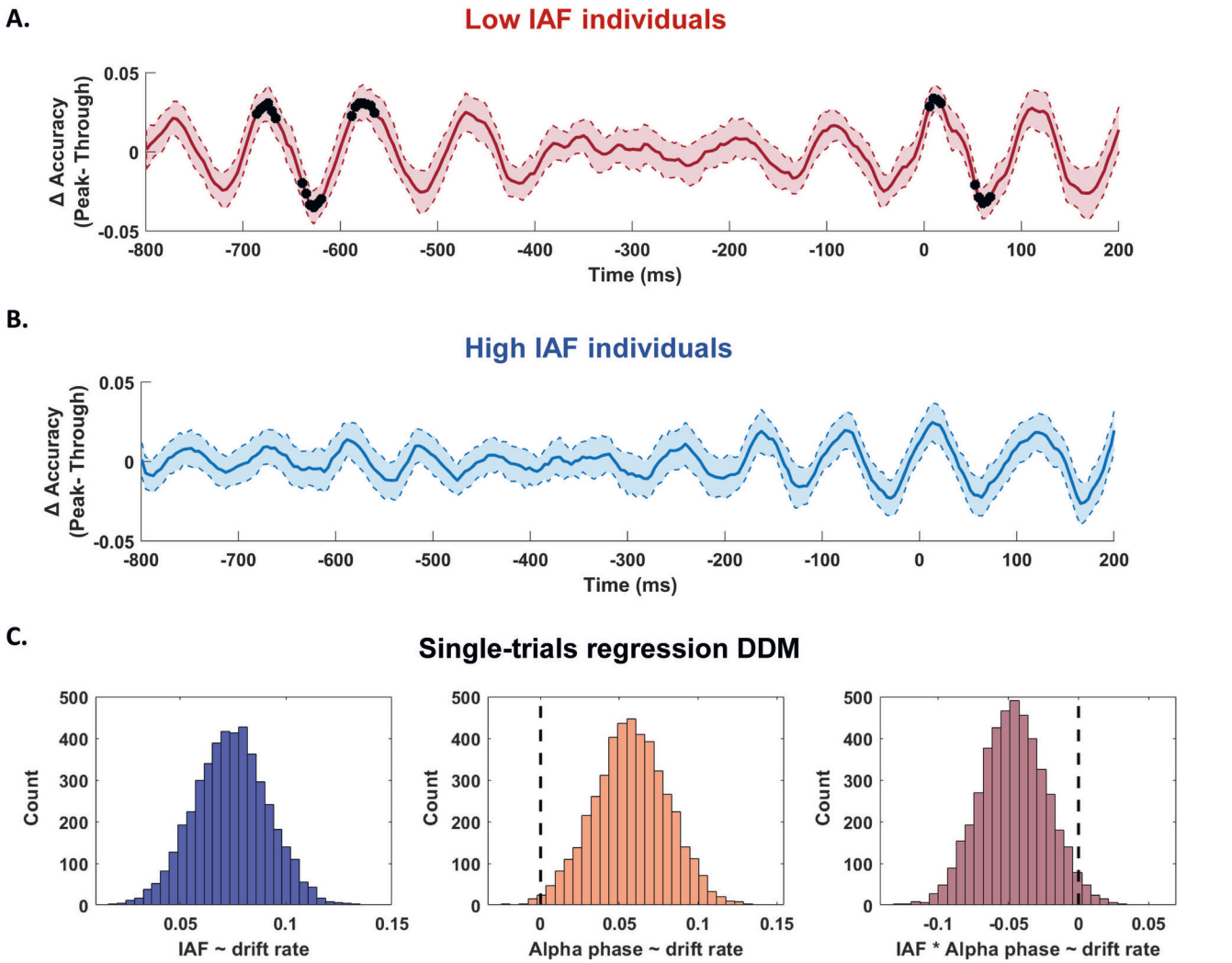

Fig. 4 | Within-subject analysis of the alpha phase effect on detection accuracy. **A** Within-subjects analysis (paired *t*-test, two-tails) of the alpha phase in the peri-stimulus time revealed a variation in the accuracy of perceptual reports depending on the relative position (peak vs. trough) of the instantaneous phase in participants belonging to the first tercile of IAF (i.e. the low IAF group, $N = 39$). Significant clusters emerged at −685 to −666 ms ($p = 0.048$), −639 to −619 ms ($p = 0.029$), −588 to −564 ms ($p = 0.030$), 5–17 ms ($p = 0.045$) and 52 to 67 ms ($p = 0.046$), indicating that phase exerted a stronger influence on performance when prestimulus IAF was relatively low. Significant time points are indicated with black asterisks ($p < 0.05$; permutation test; cluster corrected). Shaded regions denote mean ± within-subjects SE. **B** In contrast, participants within the third tercile (i.e. high IAF group, $N = 39$) did not exhibit a significant differentiation in the accuracy of their perceptual reports based on the considered alpha phase bin (paired *t*-test, two-tails). Shaded regions denote mean ± within-subjects SE. **C** Trial-by-trial DDM analyses across the entire sample ($N = 116$) revealed that both prestimulus IAF (posterior mean IAF -v coefficient = 0.071, HDI = [0.037; 0.110], $q < 0.001$) and alpha phase (posterior mean alpha phase -v coefficient = 0.064, HDI = [0.017; 0.110], $q = 0.002$) were positively associated with the drift rate. The analysis unveiled a negative interaction term between IAF and alpha phase (posterior mean alpha phase* IAF -v coefficient = −0.041, HDI = [−0.087; 0.001], $q = 0.043$). This result highlighted that the impact of alpha phase on dictating perceptual sensitivity is reduced vs. increased in the presence of higher versus lower prestimulus alpha frequency. *q*-values represent the proportion of posterior samples crossing zero.

whether correct versus incorrect responses were associated with distinct phase angles. Watson-Williams test revealed that, while no significant clusters emerged in either the whole sample or the high IAF group (Fig. 5B), the low IAF group showed a notable cluster spanning from approximately −800 ms to −300 ms (Fig. 5A). Within this interval, the phase angles associated with correct and incorrect responses significantly differed (p cluster = 0.041).

Alpha-phase clustering increases for correct responses only in low IAF individuals

To further test whether the correctness of the perceptual report was related to alpha phase, we computed intertrial phase clustering (ITPC) separately for each time point in the −800 ms to 200 ms window. In the whole sample, we observed a distinction in alpha-clustering between correct and incorrect responses ($p = 0.011$). However, we aimed to investigate whether this effect varied as a function of IAF. Given that higher IAF may reduce the impact of phase, we hypothesised that accounting for IAF could reveal a more nuanced pattern, potentially diversifying the effect based on the speed of alpha. To address this, we repeated the analysis separately for individuals with low IAF and high IAF. The results revealed a notable difference: in the high IAF group, there was no significant disparity in ITPC between correct and incorrect decisions. However, in the low IAF group, ITPC exhibited a significant differentiation ($p = 0.045$), suggesting a more pronounced influence of alpha phase on perceptual accuracy in this subgroup (Fig. 6A). To further reinforce the finding, we also computed ITPC across frequencies ranging between 2 and 50 Hz. This analysis aimed to ascertain that the previously observed effect was specifically

https://doi.org/10.1038/s41467-026-70124-9

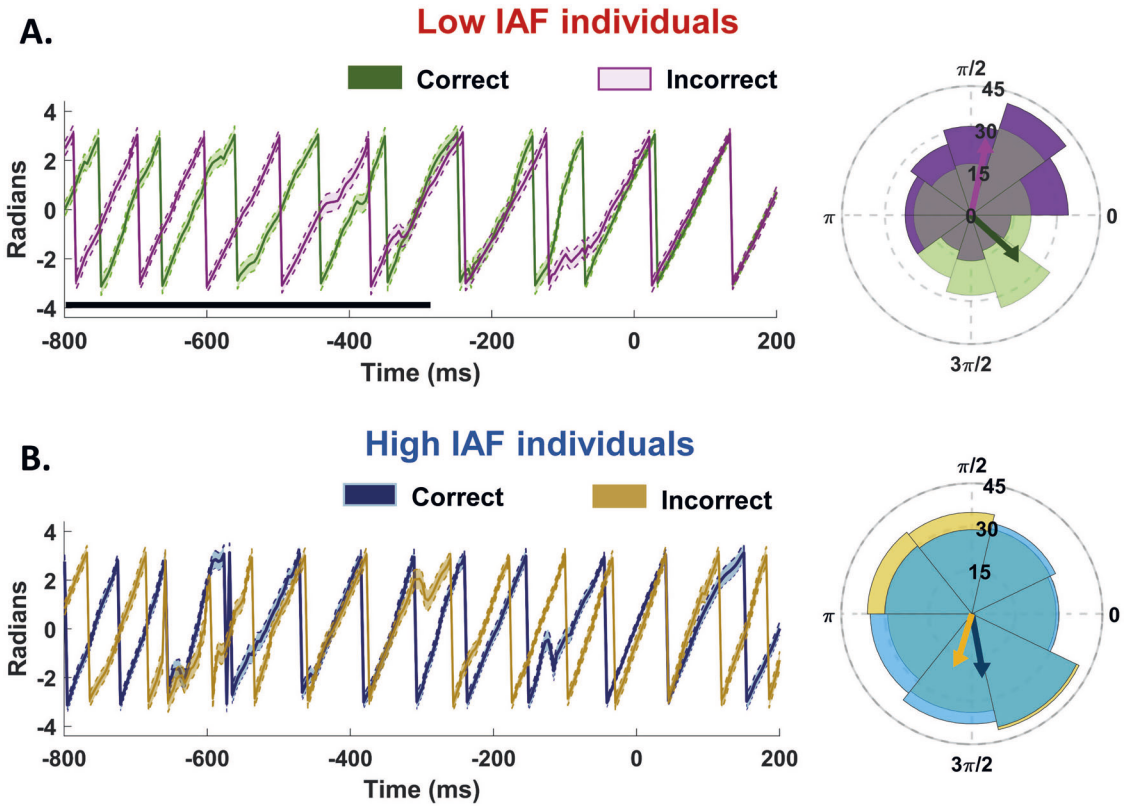

Fig. 5 | Phase angle differentiates correct and incorrect decisions in the low IAF group. A In the low IAF group ($N = 39$), a reverse data-driven analysis (left panel) identified a significant cluster from −800 ms to −300 ms, where phase angles differed significantly between correct and incorrect responses (p cluster = 0.041), indicating a phase-dependent effect on decision accuracy. Significant time points are indicated with black lines ($p < 0.05$; permutation test; cluster corrected). Shaded regions denote mean ± within-subjects SE. On the right, a polar plot shows the phase angles and the mean angle, focusing on the interval where the effect was most prominent in the binned phase angle analysis (−639 ms to −619 ms; Fig. 4A), highlighting the differences between correct and incorrect responses. **B** In the high IAF group ($N = 39$), no significant clusters were found, suggesting a lack of distinct phase angle association with response accuracy in this group. Shaded regions denote mean ± within-subjects SE. The polar plot shows that, unlike in the low IAF group, phase angles are clustered along the same angle regardless of decision outcome.

tied to the alpha-band. The results of the cluster-based analysis (Fig. 6B) revealed three findings: (1) there was an increase in ITPC in correct vs incorrect trials, (2) this effect was group-specific, holding true only for individuals with low IAF ($p = 0.038$) and (3) this effect was confined to the alpha-low beta band. These findings also held when we directly contrasted the correct–incorrect ITPC difference between groups: the increase in ITPC for correct versus incorrect perception was greater in Low-IAF than in High-IAF participants within the high-alpha/low-beta range (Fig. S8, $p = 0.043$).

Discussion

Alpha oscillations play an important role in various cognitive, perceptual and decision-making processes[7,8,24,31–36]. Specifically, the frequency of alpha oscillations has been integrated into the perceptual cycle theory[3], which conceptualises perception as a series of discrete processing epochs. Consequently, the temporal aspects of perception have been linked to the frequency of alpha oscillations, emphasising their role in periodic sampling and transmission of sensory information in both healthy[11,12,37–39] and clinical populations[40,41].

Accordingly, our results add to this body of research by indicating that IAF is associated with variations in perceptual sensitivity, as spontaneous inter-trial fluctuations in IAF relate to the accuracy of perceptual decision. The magnitude of the detected effect is consistent with earlier studies examining the link between alpha frequency and perceptual outcomes[9,16,42]. Notably, we test the hypothesis linking instantaneous alpha frequency to sensory accuracy using a multifaceted protocol that integrates classical bin-based analyses, trial-by-trial analyses and integrated computational models such as the SDT and the DDM. Moreover, to ensure that this association did not depend on the instantaneous-frequency extraction method, we conducted supplementary analyses (Supplementary Methods 5–8) based on pooled-trials spectrum peak estimation, automated frequency-detection algorithms, Gaussian fitting of aperiodic-corrected spectra and FFT-based single-trial estimation. All approaches converged on the same pattern: trials with higher alpha frequency were associated with higher perceptual sensitivity. Nonetheless, we acknowledge that instantaneous-frequency estimates inherently rely on specific signal-processing assumptions; although multiple alternative approaches yielded converging results, this aspect remains a methodological consideration for future studies.

Taken together across bin-based analyses, trial-by-trial approaches and computational modelling, this body of evidence suggests that alpha frequency is a candidate mechanism involved in shaping the accuracy of visual sampling[13,19]. This represents a basic mechanism that precedes and encompasses temporal integration processes, similarly finding a functional role of IAF in temporal binding. Indeed, the candidate mechanism identified in this study, linking alpha variations to perceptual accuracy variability, would be the same that ensures greater temporal resolution. For example, in the two-flashes fusion task[9], the opportunity provided by a higher alpha to sample the two flashes more likely in the optimal phase would lead to an increase in the capacity for correct temporal discrimination (Fig. 7), suggesting the presence of common mechanisms and neural codes that may underpin perceptual and temporal sampling.

https://doi.org/10.1038/s41467-026-70124-9

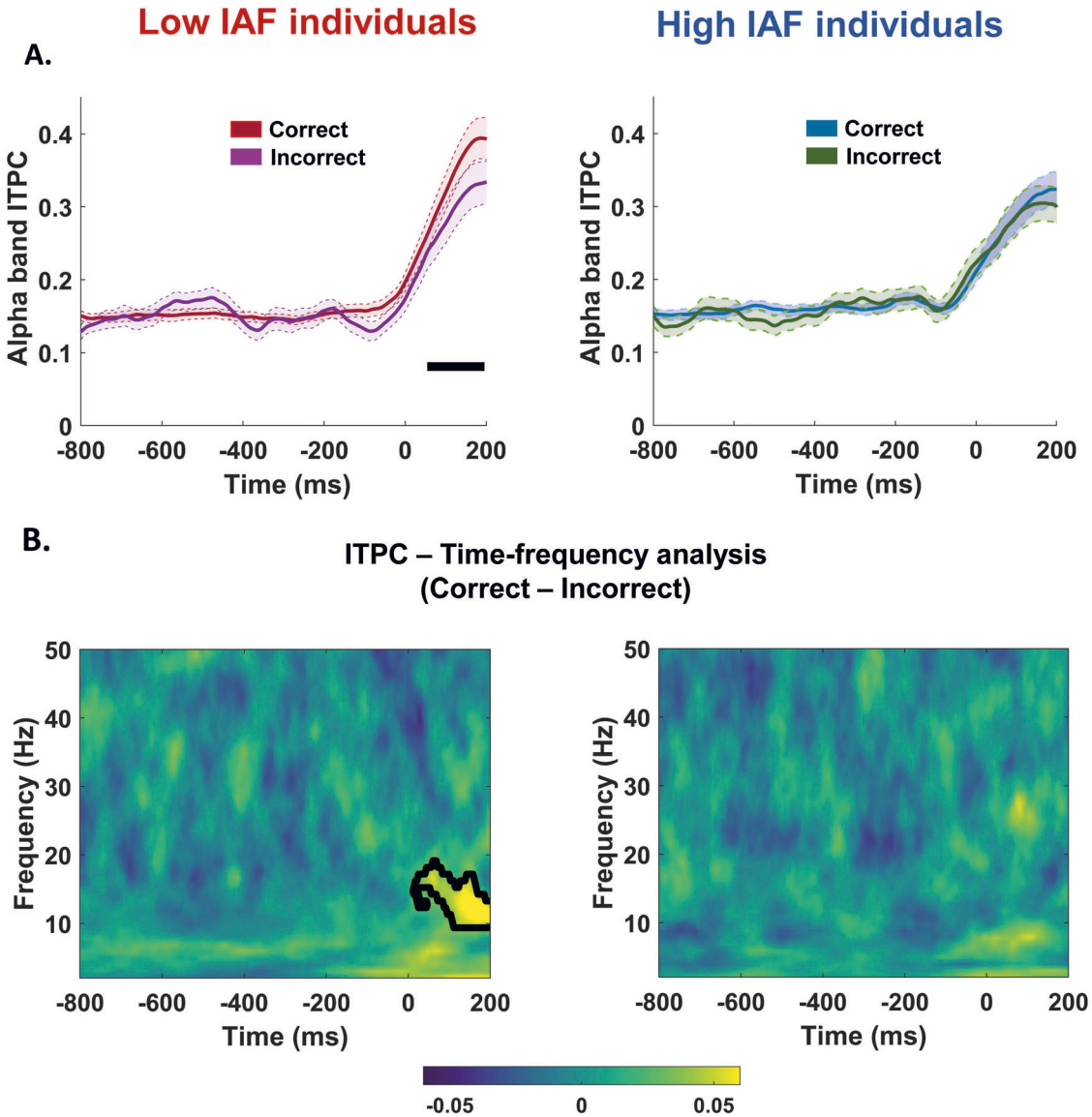

Fig. 6 | The effect of phase on perception interacts with instantaneous alpha frequency. A Intertrial Alpha phase clustering (ITPC) analysis revealed a significant difference in ITPC between correct and incorrect decisions in the peristimulus time within the low IAF group (p cluster = 0.045), while no statistical differentiation was observed in the high IAF group. Significant time points are indicated with black asterisks ($p < 0.05$; permutation test; cluster corrected). Shaded regions denote mean ± within-subjects SE. **B** An extension of the ITPC analysis across a broader time-frequency range confirmed that the observed effect was specific to the alpha-low beta band and exclusively present in individuals within the low IAF group (p cluster = 0.038). Statistically significant time–frequency points (cluster-based permutation test, $p < 0.05$) are delineated by a black contour.

In addition, the overall pattern of results indicated that there is no statistical relationship between IAF and response bias across the various analyses. However, an exception emerged in the time-resolved analysis, where higher IAF was associated with a reduction in bias compared to lower IAF. This finding points to a potentially intriguing mechanism, suggesting that high IAF could indirectly reduce bias by improving perceptual sensitivity. In this case, higher sensitivity may allow participants to detect stimuli more precisely, limiting the role of bias in their responses. Nonetheless, this effect was confined to a specific window in the time-resolved analysis and did not persist across other measures, suggesting its limited impact.

These findings prompted us to investigate how the increase in the cycling of alpha frequency contributes to an enhancement in perceptual accuracy and through which mechanism this connection operates. We hypothesised that different IAF within- and between- subjects could be linked to varying probabilities of falling into optimal phases for stimulus processing. The phase of alpha oscillations has been demonstrated to exert an influence on human perception. Specifically, stimulus detection and discrimination have been found to be determined by alpha phase[20–22,34,43]. We have been able to replicate these findings, as we identified that decisional accuracy varied depending on the alpha phase bins considered. Crucially, we have demonstrated an interaction between IAF and the phase's impact on perception. This insight emerges as the accuracy variation linked to specific alpha phase bins exclusively holds true within the subset of individuals characterised by a low pre-stimulus IAF. Furthermore, from the implemented trial-by-trial analysis, we demonstrated the presence of a negative interaction between IAF and phase. This interaction implies that in trials marked by a higher IAF, the phase exerted a diminished influence on decision accuracy. Supporting this finding, a complementary analysis—investigating whether the mean phase angle differed between correct and incorrect responses—uncovered a

https://doi.org/10.1038/s41467-026-70124-9

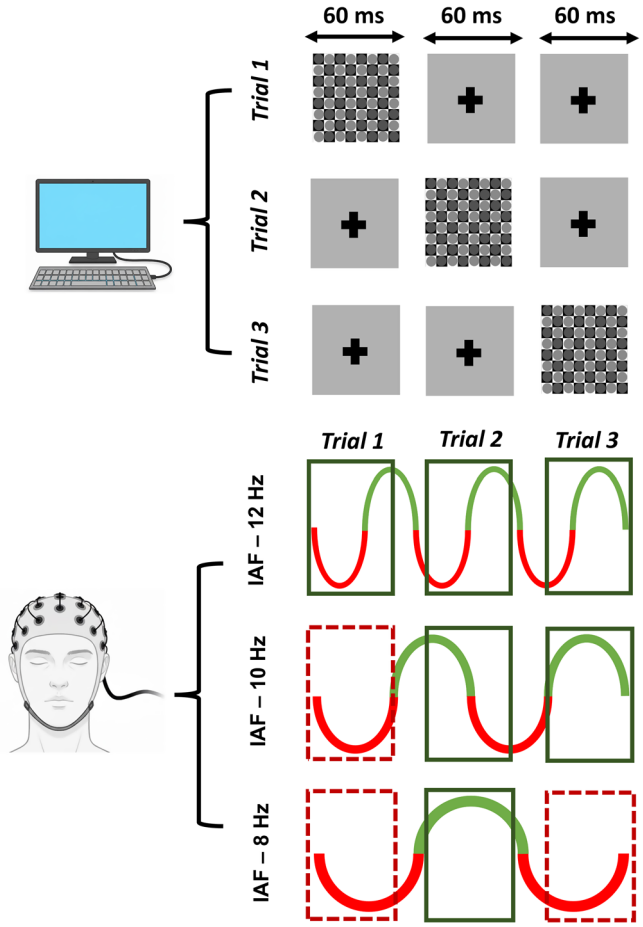

Fig. 7 | Alpha frequency shapes perceptual sensitivity through optimal alpha phase probability occurrence. The candidate mechanism that would ensure a higher IAF resulting in a more accurate sensory representation relies on the increased probability of the external signal aligning with the optimal phase for stimulus perception. The rationale is that an individual with a higher alpha frequency can navigate through a wider array of phase angles within the same timeframe compared to someone with a lower alpha frequency. To illustrate the proposed mechanism, we have represented three individuals with different IAF (12 vs. 10 vs. 8 Hz). Furthermore, we have created three different scenarios in which the stimulus is presented in a different temporal moment. Green boxes represent accurate responses, while red boxes represent wrong responses. During the stimulus presentation (59 ms), individual with higher alpha covers more ground, encountering and embracing various phase angles, while the lower alpha counterparts traverse a narrower spectrum during the identical processing window. This difference is important in understanding decision outcomes. For low IAF individuals, the time point of visual stimulus occurrence hitting a specific alpha phase angle becomes a critical factor for successful stimulus processing. This is explained by the less likely transition from an unfavourable phase bin to a favourable one precisely at the time of stimulus occurrence. In essence, the limited coverage of lower alpha diminishes the probability of aligning with optimal phases during stimulus presentation, amplifying the impact of phase positioning on decision outcomes. This conceptualisation highlights that perceptual accuracy would depend not on how long the system remains within an optimal phase, but on how many opportunities it has to align with one.

significant, group-specific effect. Specifically, only in the low IAF group did the phase angles significantly differ between correct and incorrect decisions. Finally, we showed a heightened clustering of alpha phase in individuals with lower pre-stimulus IAF in correct vs. incorrect trials, a phenomenon that is absent in those with higher alpha, where no statistical differentiation in alpha phase clustering between correct and incorrect responses is evident. Our findings underscore the importance of considering individual differences in IAF when interpreting phase-related effects. Inter-individual IAF variability is influenced by several factors, which could, in turn, modulate the IAF-phase relationship found here. For instance, the properties of the optic radiation —the primary white matter tract connecting the thalamus to the primary visual cortex—as well as genetic factors play a role in modulating individual differences in IAF[44,45]. IAF also tends to decline with age[46], and conditions such as schizophrenia or even schizotypy traits are associated with a lower IAF[40,41]. Future research should explore how these IAF-related factors might modulate the role of phase in perceptual processes, either enhancing or diminishing its impact.

But how can IAF and alpha phase interact? The core reasoning relies on the assumption that an individual with a higher alpha frequency can traverse a broader range of phase angles within the same temporal interval compared to an individual with a lower alpha frequency (Fig. 7). To illustrate, envision two individuals, one showing a relatively higher IAF and the other showing lower IAF, processing stimuli within the same timeframe. The one with higher alpha covers more 'ground', encountering and embracing a multitude of phase angles. In contrast, the lower alpha counterpart covers a narrower spectrum of phase angles during the identical processing window. This distinction becomes important in understanding decision outcomes, especially in individuals with lower IAF. For them, the positioning of the alpha phase at specific time points becomes a critical determinant: for individuals with lower alpha frequency, the transition from the unfavourable phase bin to the favourable one precisely at those crucial points is less likely. In essence, the restricted coverage of the lower alpha diminishes the probability of aligning with optimal phases during stimulus presentation, intensifying the impact of phase positioning on decision outcomes. Moreover, this effect would be amplified by the greater IAF variability observed in individuals with higher IAF during the prestimulus period. This increased variability enhances their advantage, as it allows for more dynamic phase coverage, maximising the likelihood of aligning with favourable phases during task performance and thereby optimising decision accuracy.

This reasoning also suggests that what matters may not be the absolute duration spent within an optimal phase, but rather the number of distinct opportunities the system has to align with such a phase. In other words, repeated sampling may confer a stronger benefit than prolonged single exposures, as each new cycle provides an independent chance to validate or revise the initial sensory evidence. A similar principle has been empirically demonstrated in the 2FF paradigm[9], where temporal discrimination was not enhanced by longer single perceptual episodes, but instead by the opportunity to generate two separate sampling events. Consistent evidence comes from Cecere et al.[11], who demonstrated that IAF determines the temporal window of perceptual integration, with slower alpha rhythms leading to longer integration windows and, consequently, greater temporal fusion across sensory events. Similarly, Wutz et al.[17] found that the peak frequency of alpha oscillations increased when visual task demands required temporal segregation compared with integration. Thus, a faster IAF increases not only the likelihood of 'hitting' the optimal phase at least once, but also the number of distinct samples that can be accrued within a given interval. By contrast, slower rhythms, although extending the duration of each phase, risk both missing the optimal phase altogether and relying excessively on a single, potentially misleading shot of information. Taken together, this framework aligns with the view that perceptual accuracy is optimised through multiple brief samplings rather than prolonged single exposures. We hypothesise that the alpha range may reflect a timescale compatible with circuit integration and long-range communication delays, which could increasingly hamper coherent sampling at much higher frequencies. In line with this, computational models of the visual system incorporating realistic conduction delays naturally generate alpha-like reverberations and travelling waves[32].

Moreover, this reasoning resonates with recent theories proposed by Karvat and Landau[47]. The authors noted that in tasks assessing temporal resolution, the discriminative threshold between one and two flashes falls within the range of 15–40 ms. This relatively short interval further supports the role of phase. Specifically, if temporal integration occurs within a window corresponding to one-eighth to one-fifth of the alpha cycle, stimuli would need to reach specific parts of the alpha wave (i.e. phase) to be effectively influenced by alpha oscillations. In the context of our task, this suggests that higher IAF may enable stimuli to align more precisely with these critical wave phases, thus facilitating precise detection performance. Additionally, the gradual acceleration of IAF observed in response to increasing task demands—peaking as task demands rise from rest to low-demand conditions and reaching its maximum in high-demand scenarios[48]—may reflect a mechanism that allows the brain to enhance the likelihood of re-entering optimal processing phases.

Building on this reasoning, we hypothesise that altering IAF through neurostimulation[19,49–51] or sensory entrainment protocols[39] could further validate this interaction. Specifically, increasing IAF is expected to reduce the impact of alpha phase on perceptual accuracy, while decreasing IAF might enhance the role of phase in shaping perceptual performance.

Another important aspect to consider and further investigate is the role of stimulus duration, as it could significantly influence the interaction between IAF and alpha phase. For brief stimuli—specifically those lasting less than one alpha cycle, such as those used in our study—the interaction between IAF and phase may be more pronounced compared to longer stimuli. However, another potential factor modulating this relationship is the variability of sensory input. Since the external world is inherently dynamic rather than static, the effects of IAF and phase may accumulate across this fluctuating environment. In such context, higher IAF would make it more likely to enter favourable phases, with these effects aggregating as subsequent snapshots of sensory information are integrated over time. This cumulative process could contribute to a more accurate and coherent representation of the external world. Furthermore, it is also conceivable that, even for long-lasting static stimuli, this mechanism could exert a similar influence. In these cases, the increased opportunity to accumulate more information within a given time period could enhance the statistical reliability of sensory processing, with more frequent updates facilitating a robust integration over time. Follow-up studies incorporating a range of stimulus durations will be essential to determine whether the observed phase effects are consistent across different temporal contexts, or if they are specific to the short-duration stimuli used in our study. Moreover, varying stimuli over time may offer a more complex dynamic of the interplay between IAF and phase angles, a hypothesis currently tested in our laboratory.

In addition, the interaction between IAF and phase is not the only factor that could influence the role of IAF in shaping perceptual accuracy. For instance, our data reveal rhythmic fluctuations in accuracy and sensitivity, with cycles occurring approximately every 250–300 ms (Fig. 2A, B). Interestingly, this pattern mimics the one observed in Samaha et al.[9] (see their Fig. 4), suggesting that cross-frequency coupling—particularly interactions between theta and alpha oscillations—might play a role in modulating the effect of IAF on perceptual performance[52]. While this study does not directly investigate these oscillatory dynamics, future research could explore how theta-alpha coupling influences the relationship between IAF and visual processing.

This result may have potential broad-reaching implications. For example, it provides interpretative insights into clinical and neurological conditions characterised by imprecise external representations. For example, the important slowdown of alpha oscillations observed in the schizophrenic spectrum[41,53] may be the physiological underpinning of distorted sampling of external evidence, that potentially facilitate the establishment of distorted representations that, in turn, could exacerbate positive symptoms[54–59]. Related to this point, the results suggest the idea that modulating IAF through neurostimulation[11,15,19] as well as sensory entrainment[39] could be a useful mean to enhance the fidelity of conscious representation of the external world with potential clinical and research applications. Follow-up studies combining such causal manipulations with computational modelling will be essential to clarify how experimentally induced changes in alpha frequency shape perceptual computations and to delineate the mechanistic pathways suggested by the present findings.

Furthermore, our findings help clarify the interplay between alpha phase and perception and also offer a possible explanation that could elucidate the reasons behind studies reporting null results in this relationship[60–62]. We posit that the divergence in findings may arise from a frequently overlooked factor—individual differences in IAF. The nuanced interplay we unravelled between IAF and alpha phase implies that the speed at which alpha oscillations occur plays an important role in determining how phase influences perceptual decisions. Thus, this intricate relationship uncovered introduces a perspective that holds the potential to harmonise seemingly conflicting results within the current literature. Whereas past studies may have struggled to highlight a direct link between alpha phase and perception, our research suggests that IAF could serve as a crucial moderator, shaping both the strength and nature of this association. Disregarding this essential variable could obscure the actual relationship between alpha phase and perceptual accuracy. Additionally, this evidence aligns with studies suggesting that the explanatory power of brain rhythms on behaviour is enhanced when combining multiple oscillatory indices, rather than examining them separately. For instance, Fakche et al.[63] provide compelling causal evidence demonstrating that the effect of alpha phase on TMS-induced phosphenes is more pronounced during high alpha amplitude trials, while it is less influential during low alpha amplitude trials. Additionally, integrating aperiodic components could offer further insights. For example, Deodato and Melcher[64] have shown that, alongside alpha frequency, the aperiodic component also impacts performance in the flash fusion task. Moreover, follow-up studies could investigate the relationship between eye movements and IAF-related effects, as several recent and influential theories suggest a link between alpha activity and eye-related activity[65]. For example, analysing how blink-related ICA components interact with the effects we highlighted could provide valuable insights.

In conclusion, our study provides insights into the interplay between IAF and perceptual decision-making. We confirmed the role of IAF in shaping perceptual accuracy, demonstrating that trials with higher IAF were associated with higher sensitivity and accuracy. Importantly, our approach, integrating large-scale analyses, Bayesian statistics, and computational modelling (i.e. DDM), supports the robustness of the IAF–behaviour relationship. Furthermore, we uncovered an inter-relationship between IAF and alpha phase, which suggests a candidate mechanism through which IAF may influence perceptual decisions. The interaction suggests that the speed of alpha oscillations determines the extent of phase angles covered within the same timeframe, impacting the alignment with optimal phases crucial for accurate perception. As a result, these mechanisms intricately collaborate to shape a faithful (or not) representation of the perceptual environment. The potential for selectively modulating these oscillatory processes through non-invasive neurostimulation and sensory entrainment provides a foundation for future translational neuroscience approaches and holds promise for diverse clinical applications.

Methods

Participants

125 individuals (70 female; age range 18–35) participated in the study. All participants signed a written informed consent prior to taking part

in the study, which was conducted in accordance with the Declaration of Helsinki. The protocol was approved by the Bioethics Committee of the University of Bologna (protocol code 201723, approved on 26 August 2021). All participants had no neurocognitive or psychiatric disorders. The identified results were aggregated across both genders. Gender was determined based on participants' self-reports. We did not conduct separate analyses by gender because previous literature did not report a gender effect on the neural markers (i.e. IAF), nor on the detection task we focused on. No statistical method was used to predetermine sample size; however, we aimed to recruit a relatively large sample to ensure stable estimates of inter-individual variability and to increase the reliability of trial-level analyses.

Experimental procedure

Stimuli were presented on an 18" CRT display (Cathode Ray Tube, CRT, display resolution of 1280 × 1024 pixels, refresh rate 85 Hz) at a distance of ~57 cm in a dimly lit room. Participants sat in a comfortable chair in front of the monitor. The stimuli were generated and presented using MATLAB (version 2016, The MathWorks Inc., Natick, MA) and the Psychophysics toolbox. Visual stimuli were checkerboards appearing on the lower left visual field. The checkerboards presented could contain grey circles within each of the cells (target) or not (catch trials). Stimuli had spatial frequency of 5.16 cycles/degree, and they were presented only in the lower part of the screen at 4.1°/3.7° eccentricity (horizontal/vertical). Each black and white checkerboard was flashed for 59 ms. Participants were instructed to indicate via the keyboard the presence (key 'k') or absence (key 'm') of the grey circles inside the checkerboard. Following a training phase, each participant underwent a staircase procedure to determine the contrast level of the grey circles needed to achieve 70% detection accuracy. This procedure was conducted with an equal number of target-present and target-absent trials. Specifically, participants completed blocks consisting of five trials with targets present and five trials with targets absent. After each block, the participant's accuracy was assessed. If the accuracy was 50% or lower, the grey contrast was increased by 4 points. If the accuracy was below 70%, the contrast was increased by 1 point. Conversely, if the accuracy was 90% or higher, the contrast was decreased by 4 points, and if it was above 70%, it was decreased by 1 point. This procedure was repeated 25 times. The stimuli used included checkerboards with grey circles embedded, with the lowest contrast being red, green and blue (RGB) values of 15/240 (where the first value refers to the contrast of the circles against the white squares and the second value against the black squares) and the highest contrast being 75/180. The initial contrast for threshold estimation was set between these two extremes (RGB value: 45/210). The detection threshold was estimated based on the final three blocks. Including target-absent trials was needed for obtaining a bias-free measure, avoiding confounding effects related to participants' decision criteria. Without target-absent trials, it would be difficult to determine if variations in threshold values were due to actual perceptual ability or simply the number of hit rates, despite equal sensitivity when controlling for false alarms[66]. This approach aligns with the SDT principle, where d' is calculated by considering both hit rates and false alarms to derive a bias-free measure of performance. The bias-free approach means that, assuming equal sensitivity, the choice of a liberal or conservative decision criterion does not affect the estimation of the contrast threshold, unlike classical staircase methods (e.g. two-down, one-up methods; Levitt[67]). Notably, this threshold estimation method was first implemented in Tarasi et al.[24] and in Tarasi et al.[25]. The second phase comprised 180 trials (Fig. 1). Each trial started with the appearance of a neutral cue presented at the centre of the screen. The cue was presented for 1 s followed by a fixation dot. After a variable delay of 1.2–1.5 s a checkerboard containing (or not) grey circles at the titrated contrast within it appeared at the bottom left of the monitor for 59 ms. After collecting the response, the screen appeared black for 1.9–2.4 s in the inter-trial interval. We opted to present the stimulus in only one hemifield to prevent spontaneous fluctuations in attention between the two hemifields in the prestimulus period from interfering with the results. Participants had to determine the presence or absence of the grey circles within the checkerboard and press the button associated with their choice. No timeout was set for the response.

EEG acquisition and analysis

We used a Brain Products actiCHamp EEG amplifier with 64 channels, configured according to the international 10–10 system. EEG was measured with respect to FCz electrodes, and all impedances were kept below 10 kΩ. EEG signals were acquired at a rate of 1000 Hz. EEG was processed offline with custom MATLAB scripts (version R2021a) and with the EEGLAB toolbox[68]. The EEG recording was filtered in the 0.5–100 Hz band and a notch-filter at 50 Hz was applied. The signals were visually inspected, and noisy channels were spherically interpolated. Then, trials containing excessive noise, muscle or ocular artefacts were discarded. An average of 149 trials per subject passed this stage. Next the recording was re-referenced to the average of all electrodes, and the Independent Component Analysis (ICA) was applied. On average, 6.4 ± 0.38 components were removed, primarily those associated with eye movements, blinks, muscle artifacts and noisy electrodes. The signal was downsampled to 256 Hz.

Extract instantaneous alpha frequency and phase

The instantaneous alpha frequency was extracted following the methodology described in ref. 69 and further extended in ref. 70. First, we took the derivative of the time-series data[71] in order to remove the aperiodic component in the data, which could introduce bias in frequency estimation[70] (the same IAF–accuracy patterns emerged using alternative aperiodic removal method, Supplementary Method 9). Next, for each participant, we selected the occipital electrode signal (Oz, O2, POz, PO4, PO8) showing the highest alpha power (7–13 Hz) in the pre-stimulus time (from −800 to −100 ms) computing using the EEGlab spectopo function[68]. We focused the analysis on the occipito-parietal electrodes on the midline and right side, given that the stimulus was always presented on the left. We then applied peak-detection algorithms developed by ref. 72 to check the presence of a peak in the chosen electrode. In cases where no peak could be identified, we selected subsequent electrodes displaying higher alpha power. Participants without detectable peaks in any of the electrodes considered were excluded from further analysis, as the absence of peak in the power spectrum could bias frequency sliding to non-frequency shift features[70]. After these preliminary steps, the participant count reduced to 116, with 9 individuals removed. The distribution of selected electrodes was as follows: Oz (11%), POz (25%), O2 (11%), PO4 (22%) and PO8 (31%). Subsequently, we filtered the signal with a zero-phase, plateau-shaped, band-pass filter with 15% transition zones (MATLAB function filtfilt.m) centred on the individual oscillation peak extracted in the previous stage (filter range from IAF-2 Hz to IAF + 2 Hz). Then, a Hilbert transform was applied to the filtered data (MATLAB function hilbert.m) to extract phase angle time series. The instantaneous frequency was obtained by calculating the temporal derivative of the instantaneous phase. We reduced the noise present in the instantaneous frequency by median filtering ten times the instantaneous frequency using ten different time windows ranging from 10 to 400 ms. Additionally, we adopted complementary approaches to examine the role of IAF without relying on the instantaneous frequency method, instead using FFT-based frequency estimation. First, we computed the power spectrum from the pre-stimulus signal (−800 to −100 ms), matching the time window used for the instantaneous frequency approach. We then applied Corcoran's algorithm to the single-trial power spectra to extract the single-trial IAF. This peak detection method, performed directly on the frequency spectrum, helps overcome potential limitations of the instantaneous frequency

approach[70,73]. We also implemented a Gaussian fitting approach: for each trial, we fitted a Gaussian to capture the spectral peak within the alpha band. The centre frequency of this Gaussian was taken as the IAF. These methods together confirm the relationship between IAF and perceptual performance.

IAF binning analysis across pre-stimulus time

To evaluate the effect of pre-stimulus IAF in directing decisional outcome, we employed a binning analysis using an approach similar to the one employed by ref. 18. Specifically, for each individual, trials were sorted into three terciles according to the instantaneous frequency (i.e. first-IAF, second-IAF and third-IAF trials), independently for each pre-stimulus time point. Then, the SDT parameters indexing perceptual sensitivity (d') and bias (c) were computed separately for the first and the third terciles. d' reflects standardised measure of discrimination abilities between the signal and the noise and was calculated as $d = z(HR) - z(FA)$, where z represents the z-scores of Hit rate (i.e. HR, the probability of correct response on target trials) and false alarms (i.e. FA, the probability of incorrect response on catch trials). Conversely, c quantifies a subject's decision criterion (i.e. c value over 0 implies the presence of a bias to report the absence of the target) and was calculated as $c = \frac{-z(HR)+z(FA)}{2}$. To ensure a proper estimation of d' and c, we corrected the extreme rates of hit and false alarm. Rates of 0 were replaced with $\frac{(0.5)}{n}$, and rates of 1 were replaced with $\frac{(n-0.5)}{n}$, where n is the number of signal or noise trials[74] To statistically assess whether the SDT parameters differed as a function of the bins considered, we entered d' and c indices extracted across pre-stimulus time into a cluster-based statistic. The real cluster size was obtained by summing t-values (exceeding an alpha threshold of 0.05) of two-sided paired t-tests over adjacent time points. The null hypothesis distribution of the cluster sizes was drawn by randomly shuffling ($n = 1000$), across participants, the association between SDT parameters (i.e. d' and c) and bins (first vs. third IAF terciles) and choosing the maximum cluster value (i.e. summed t-values in significant adjacent points) per each randomisation. From this dummy distribution, we have extracted the cluster size corresponding to the 95% percentile and we compared the actual cluster size with this statistical threshold. The same statistical procedure was repeated using accuracy as a dependent variable. We calculated the p-value for each cluster by determining the position of the observed clusters within the distribution of clusters generated from the permutation procedure. This approach was applied consistently across all permutation-based analyses. To ensure the validity of our findings, we conducted additional analyses to verify the consistency of our results across different bin configurations. Initially, we expanded our primary analysis to include the second IAF bin and performed ANOVA on accuracy, d', and criterion measures across the three IAF bins. This approach allowed us to assess whether the differences observed remained significant when including the second bin, rather than just focusing on comparisons between the first and third bins. In addition, we conducted regression analyses to assess whether there was a monotonic trend in accuracy and d' across the three bins, which would suggest a gradual increase in performance with higher IAF (Supplementary Method 1). To further validate our findings, we also explored the impact of different bin configurations. Specifically, we divided the trials using two and four bins. For the two-bin configuration, trials were divided into above-median and below-median IAF bins. A paired t-test was used to compare accuracy and d' between these two trials type. For the four-bin configuration, we divided trials into quartiles and assessed performance measures across these quartiles.

IAF binning analysis collapsing pre-stimulus time

In an additional analysis, we averaged IAF across pre-stimulus time (−800 to −100 ms) and we then binned trials into terciles. This procedure was conducted separately for each individual. Then, we entered d', c and accuracy extracted in the first vs. third IAF terciles into both a classic paired t-test and Bayesian paired t-tests to assess whether a significant difference in SDT parameters emerged depending on the considered bins. The same analysis was then repeated using the IAF estimated from the single-trial Corcoran-derived measures. Bayesian analysis utilised the default prior settings: Prior Distribution for Effect Size: Cauchy, with a Scale Parameter of 0.707. We used these parameters for all the Bayesian test-t performed. To assess the robustness of these results, we repeated Bayesian test-t using a more conservative prior (scale = 0.5), which yielded Bayes factors that were highly similar to those obtained with the default prior. We further examined whether RT varied between the first and third terciles of trials and how these variations related to response accuracy (Supplementary Method 2). Specifically, using paired t-test, we compared RTs in the first tercile with those in the third tercile, both overall and separated by response accuracy.

IAF binning analysis: correct vs error trials

To further validate the previous findings, we employed a different approach including IAF as the dependent variable. In this analysis, we categorised the trials based on their accuracy (correct vs. incorrect trials) and investigated whether a difference in instantaneous frequency emerged based on the correctness of the response. Correct trials encompassed both correctly detected target trials (hits) and correctly detected catch trials (correct rejections). On the other hand, error trials included missing of the target in target-presence trials (miss) and target reporting in catch trials (false alarms). We then calculated the mean pre-stimulus IAF preceding correct and incorrect trials for each participant. To assess the statistical difference between IAF for correct vs. incorrect trials, we utilised both classic paired t-test and Bayesian paired t-test. These complementary statistical approaches allowed us to thoroughly examine the potential variations in IAF in relation to the accuracy of the response. In order to check that different trials count between correct and incorrect response inflated the difference between IAF extracted from correct and incorrect responses, we used a subsampling procedure to match the number of correct and incorrect trials. Specifically, for each participant, we shuffled the trials with correct responses and matched them with IAF values count from the incorrect responses. For each permutation, we calculated the average IAF for the correct responses. This permutation procedure was repeated 1000 times to ensure reliability. We then averaged the surrogate IAF values obtained from these permutations. Finally, we compared the average IAF values for correct versus incorrect responses. This comparison corroborated the initial analysis presented in the manuscript, where all trials were included as correct trials were associated with higher IAF values ($IAF_{correct} = 11.35 \pm 0.01$) compared to incorrect trials ($IAF_{incorrect} = 11.30 \pm 0.01$, $t_{115} = 4.12$, $p < 0.01$). Finally, we employed classical FFT-based approaches to confirm the presence of IAF differences between correct and incorrect responses. First, we computed the power spectrum separately for correct and incorrect trials by pooling the pre-stimulus signal within each condition. This method avoids estimating IAF at the single-trial level, ensuring a more consistent assessment of the frequency spectrum. After computing the individual power spectra for correct and incorrect responses, we identified the alpha peak using two approaches. The first, a more traditional method, involved visually detecting the alpha peak, which was not reported if no clear peak was present. In parallel, we applied a similar analysis using Corcoran's algorithm, providing a bias-free, automated and data-driven estimation of the alpha peak. Finally, we compared whether IAF differed significantly between correct and incorrect trials.

IAF single-trial regression: accuracy

To relate single-trial estimates of instantaneous frequency to single-trial accuracy, we used a non-parametric multiple regression approach

similar to that described in refs. 26,28. Specifically, a regression coefficients describing the relationship between prestimulus IAF and accuracy were estimated according to the following linear model $\beta = (X^TX)^{-1}X^TD$ where X represent a design matrix containing one column for the intercept (all 1 s), one column of IAF (each row represented the average IAF observed in the pre-stimulus time in that particular trial), whereas D is the vector of accuracy scores (dummy coded as 1 or 0). The resulting β coefficients describe the contributions of IAF in explaining accuracy. First, we averaged the IAF across the prestimulus window (−800 to −100 ms) and then applied z-scoring to reduce the impact of outlier values, and β was estimated using a least-squares solution. β coefficients were then converted into a z-score relative to a subject-specific null hypothesis distribution obtained by repeatedly shuffling ($n = 2000$) the mapping between the accuracy values and the IAF values. The coefficient associated with the true data mapping was subsequently transformed into a z-statistic, relative to the mean and standard deviation of the permuted data. According to this approach, it is possible to weight the variability (i.e. noise) present at the subject-level into the subsequent group-level analyses[28]. Because the null hypothesis claims that there is no relationship between IAF and accuracy (i.e. $\beta = 0$), we conducted a test-t against 0 to assess the statistical significance of the observed β coefficients. In order to get information on the strength of the effect, we also investigate this effect using a Bayesian test-t. We then tested whether the results of this analysis were confirmed when using IAF estimates derived from an FFT-based approach, such as the one proposed by Corcoran et al.[72], instead of single-trial IAF estimates obtained through the instantaneous frequency analysis. To corroborate the results, we examine the relationship between IAF and task accuracy by means of a generalised linear mixed model (GLMM, Supplementary Method 10). The dependent variable was task accuracy, coded as a binary variable (0 or 1). The normalised alpha frequency was used as a continuous predictor. To account for inter-individual variability, participants were included in the model as a random effect. The specific formula used for the model was accuracy~IAF+(1|Subject). MATLAB's fitglme function was used to fit the model to the data, specifying a binomial distribution and a logit link to reflect the binary nature of the accuracy data. We also analysed whether fluctuations in RT could be predicted by trial-by-trial IAF modulations. To test this, we repeated the very same regression approach described above, including RT instead of accuracy as a dependent variable.

IAF single-trial regression: drift diffusion model

We fit participants' decision using the DDM, the most widely used computational model of two-alternative decision-making tasks[23,24]. The DDM formulation we employed allows for trial-by-trial analysis, enabling us to examine the influence of individual trial characteristics on decision-making—something not feasible with SDT's reliance on aggregated data. Additionally, by using both DDM and SDT, we achieve a form of conceptual replication, strengthening our findings across different analytical frameworks. We used the HDDM package provided by ref. 75. Here, Bayesian inference through Markov chain Monte Carlo sampling is utilised to approximate posterior distributions for model parameters at both the individual and group levels. This approach is advantageous as it effectively manages the uncertainty associated with parameter estimates, allowing for robust and precise parameter estimation. The priors for each parameter in HDDM are informed by a pool of 23 studies, which report the best-fitting parameters of the DDM across various decision-making tasks[76]. By grounding these priors in empirical data, HDDM ensures that initial parameter assumptions are reliable and informed by a substantial body of existing research (see the supplement by ref. 75 for a visual representations of these priors). Using this package, we estimated regression coefficients[75] to determine the relationship between trial-to-trial variations in IAF and DDM parameters v (the rate of evidence accumulation, the so-called drift rate), z (the starting point of the accumulation process), a (the boundary separation between the two decisional thresholds) and t (non-decision time). The resulting coefficients describe the contribution that trial-by-trial fluctuations in IAF play in modulating the DDM parameters. IAF values were z-scored to mitigate the influence of outlying trials. We initialised HDDM to draw 5000 posterior samples with the first 500 samples discarded as burn-in. We removed trials with reaction times exceeding 4 s and falling below 100 ms before fitting procedure. We inspected traces of model parameters and their autocorrelation to ensure that the models had properly converged. We examined the overlap of the posterior distributions for the estimated parameters with zeros, defining significance as less than 5% overlap. Because these are comparisons of Bayesian posterior distributions, we report the HDDM outcomes as q- rather than p-values.

Assessing the specificity of the relationship between IAF and perceptual accuracy relative to alpha power

To ensure that the effects observed in relation to IAF were not confounded by oscillatory power, we conducted several analyses (See Supplementary Fig. S1–S5). First, we extracted time-frequency oscillatory amplitude maps from the aperiodic-free EEG signal. All time–frequency analyses were performed at the subject-specific electrode used for IAF estimation. Time-frequency decompositions were performed using complex Morlet wavelets for 50 linearly spaced frequencies ranging from 2 Hz to 50 Hz. Wavelets with 3 cycles at the lowest frequency and 11 cycles at the highest frequency were applied. After obtaining the absolute value of the resultant analytic signal, we conducted a cluster-based permutation test (1000 permutations, two-sided, $p < 0.05$) to evaluate whether oscillatory amplitude varied based on response accuracy (correct vs. incorrect trials) in the prestimulus period (−800 ms, −100 ms). Amplitude was baseline-normalised in dB (−3200 ms, −2800 ms relative to stimulus onset) for correct and incorrect trials. Clusters were defined as contiguous suprathreshold samples ($p < 0.05$) in the 2D time–frequency space, observed clusters were considered significant if their size exceeded the 95th percentile of the null distribution of maximum cluster sizes. Next, we extracted trial-by-trial baseline-normalised amplitude from the time-frequency analysis, averaging it within the −800 ms to −100 ms window, at the frequency bin closest to each participant's previously determined IAF. We then performed regression analyses, incorporating both trial-by-trial fluctuation in IAF and alpha power as predictors of perceptual accuracy. Both variables were z-scored within-subject. This analysis allowed us to determine whether the influence of IAF on performance was independent of alpha power. We also replicated a bin-based analysis by dividing trials into terciles based on the previously extracted baseline-normalised trial-by-trial alpha amplitude (averaged over −800 to −100 ms). We compared SDT metrics across the lowest and highest terciles to confirm that the effects observed with IAF did not hold when considering variations in alpha power. Lastly, using the same time–frequency parameters and baseline normalisation as above, we compared prestimulus power maps between low and high IAF groups via a cluster-based permutation test (1000 permutations), randomly reassigning participants to groups on each permutation while preserving group sizes. Clusters were defined as contiguous suprathreshold samples ($p < 0.05$) in the 2D time–frequency space, observed clusters were considered significant if their size exceeded the 95th percentile of the null distribution of maximum cluster sizes.

Alpha phase—binning analysis

To evaluate the effect of alpha phase in directing decisional outcome, we employed a binning analysis (for a similar approach[77–79]). Specifically, for each individual, trials were sorted into two bins according to the instantaneous phase (i.e. 0°–180° vs. 180°–360°), independently for each time point (−800 ms to 200 ms). We chose to extract two bins in order to have a sufficient number of trials on which perform the

subsequent analysis. To statistically assess whether the perceptual reports differed as a function of the bins considered, we entered accuracy index extracted across selected time window into a cluster-based statistic. The real cluster size was obtained by summing *t*-values (exceeding an alpha threshold of 0.05) of two-sided paired *t*-tests over adjacent time points. The null hypothesis distribution of the cluster sizes was drawn by randomly shuffling ($n = 1000$), across participants, the association between accuracy and bins and choosing the maximum cluster value (i.e. summed *t*-values in significant adjacent points) per each randomisation. From this dummy distribution, we have extracted the cluster size corresponding to the 95% percentile and we compared the actual cluster size with this statistical threshold. In a follow-up analysis, we have investigated whether the weight of alpha phase bin in directing the accuracy of the report could be different as a function of IAF. To this end, we portioned our original sample of 116 participants in terciles based on the mean pre-stimulus IAF they showed, selecting the first (i.e. low IAF individuals, $n = 39$) and third (i.e. high IAF individuals, $n = 39$) terciles. Finally, we computed the above-mentioned analysis separately in the two extracted groups. The two groups categorised based on IAF did not show differences in oscillatory amplitude, either in alpha or in other frequency bands (Fig. S5).

Alpha phase−single-trial regression

To relate single-trial estimates of instantaneous phase to single-trial accuracy as well as to investigate the interaction between instantaneous alpha phase and instantaneous alpha speed, we used a non-parametric multiple regression approach similar to the one used above. Specifically, regression coefficients describing the relationship between (1) IAF and accuracy, (2) alpha phase and accuracy and (3) the interaction between IAF and alpha phase were estimated according to the following linear model $\beta = (X^T X)^{-1} X^T D$. X represent a design matrix containing one column for the intercept (all 1 s), one column of IAF (each row represented the average IAF observed in the pre-stimulus time in that particular trial), one column of phase (dummy coded as 1, if in that trial the phase fell within the 0°–180° space, or 0, if in that trial the phase fell within the 180°–360° space) and one column representing the interaction between IAF and alpha phase. D is the vector of accuracy scores (dummy coded as 1 or 0). The resulting β coefficients describe the contributions of IAF, phase and their interaction in explaining trial-by-trial variation in accuracy. IAF values were z-scored to mitigate the influence of outlying trials. We chose to extract the phase in the first time-point in which we found a significant impact on phase on accuracy according to the previously bin-analysis statistic conducted. β was estimated using a least-squares solution and they were then converted into a z-score relative to a subject-specific null hypothesis distribution obtained by repeatedly shuffling ($n = 1000$) the mapping between the accuracy values and the predictors. We then conducted a test-*t* against 0 to assess the statistical significance of the observed β coefficients and we also compute the Bayesian factor.

Furthermore, we have expanded our investigation in order to evaluate whether these relationships held valid in the DDM framework. To this end, we estimated regression coefficients to determine the relationship between trial-to-trial variations in IAF, alpha phase and their interaction with DDM parameters v, z, a and t. The resulting coefficients describe the contribution that trial-by-trial fluctuations in the predictors play in modulating the DDM parameters. We initialised HDDM to draw 5000 posterior samples with the first 500 samples discarded as burn-in. We removed trials with reaction times exceeding 4 s and falling below 100 ms before fitting procedure. The statistical significance of the regression coefficients was assessed using a procedure similar to that used in the previous DDM regression analysis. Specifically, we inspected traces of model parameters and their autocorrelation to ensure that the models had properly converged, and we examined the overlap of the posterior distributions for the estimated parameters, defining significance as less than 5% overlap with the zeros value.

Watson-Williams test for phase difference between correct and incorrect choices

To investigate whether accurate and inaccurate perceptual decisions are associated with different phase angles, we analysed phase data across timepoints ranging from −800 to 200 ms. Specifically, we aimed to determine if the phase angles differed as a function of decision accuracy using the Watson-Williams test. This test, the circular analogue of the *t*-test, evaluates whether two samples of phase angles (corresponding to correct vs. incorrect decisions) are drawn from different distributions[80]. The Watson-Williams test accounts for both the mean phase angle and the circular variance within each sample, making it well-suited for analysing phase differences in electrophysiological data[81–84]. To assess the significance of phase differences, we employed a permutation-based analysis. For each timepoint where the Watson-Williams test indicated a significant difference in phase angles between correct and incorrect decisions, we calculated the corresponding *F*-value and summed these values across contiguous significant timepoints. We then compared the observed clusters of *F*-values with a null distribution of clusters generated by permuting the association between phase angles and decision outcomes 1000 times (i.e. shuffling the phase angle-accuracy relationship). This approach allowed us to determine whether the observed clusters were significantly larger than those expected under the null hypothesis. The analysis was performed on the entire sample, as well as separately for the low and high IAF groups, to explore potential differences between these groups.

Intertrial phase clustering (ITPC) analysis−instantaneous alpha phase

We computed ITPC separately for correct trials and for incorrect trials using the same instantaneous alpha phase data that were used in all other analyses. ITPC is a measure of the phase consistency across trials at a given time point, and it varies from 0 to 1, where 0 corresponds to no phase clustering and 1 to perfect clustering across trials. For each subject, ITPC values were calculated separately for correct and incorrect trials. To ensure that our observation would not be biased by the different number of correct vs incorrect trials, we conducted a resampling analysis in which trials were randomly sampled from each condition so that the minimum number of trials in each condition was matched within each subject (similar to ref. 82). This procedure was iterated 500 times to ensure that all trials were used and that reliable estimates were obtained. To statistically assess whether there was a significance difference in phase clustering between correct vs. incorrect choices, we entered ITPC index extracted across the −800 to 200 ms time window into a cluster-based statistic. The real cluster size was obtained by summing *t*-values (exceeding an alpha threshold of 0.05) of two-sided paired *t*-tests over adjacent time points. The null hypothesis distribution of the cluster sizes was drawn by randomly shuffling ($n = 1000$), for each participants, the association between accuracy and ITPC and choosing the maximum cluster value (i.e. summed *t*-values in significant adjacent points) per each randomisation deriving from two-sided paired *t*-tests run on the permuted data. From this dummy distribution, we have extracted the cluster size corresponding to the 95% percentile and we compared the actual cluster size with this statistical threshold. After conducting this analysis considering the whole sample, we repeat this analysis separately in the low vs. high IAF group.

Intertrial phase clustering (ITPC) analysis−time-frequency decomposition

To corroborate the frequency-specificity of the effect, we have also computed ITPC at frequencies between 2 and 50 Hz, separately for the

low vs. high IAF groups. Time-frequency decompositions were performed for 50 linearly spaced frequencies between 2 Hz and 50 Hz, extracted from epochs spanning −100 to 200 ms centred on target onset and using wavelets of 3 cycles at the lowest frequency to 11 cycles at the highest frequency. After extracting the angle of the resultant analytic signal, we computed ITPC for each frequency and time points. As before, we equate the number of trials when computing ITPC for correct and incorrect trials per each participant. Then, we investigated, separately for the low vs. high IAF group, whether there was a significant difference in the ITPC value between the two conditions by mean of cluster-based statistics.

Data availability

Behavioural data, preprocessed EEG, and source data underlying the findings of this study are publicly available on the Open Science Framework (OSF) at https://doi.org/10.17605/OSF.IO/6298N. Source data are provided with this paper.

Code availability

The code supporting the findings of this study are publicly available on the Open Science Framework (OSF) at https://doi.org/10.17605/OSF.IO/6298N.

References

1. Pöppel, E. A hierarchical model of temporal perception. *Trends Cogn. Sci.* **1**, 56–61 (1997).
2. VanRullen, R. Perceptual Cycles. *Trends Cogn. Sci.* **20**, 723–735 (2016).
3. VanRullen, R. & Koch, C. Is perception discrete or continuous?. *Trends Cogn. Sci.* **7**, 207–213 (2003).
4. Varela, F. J., Toro, A., John, E. R. & Schwartz, E. L. Perceptual framing and cortical alpha rhythm. *Neuropsychologia* **19**, 675–686 (1981).
5. Kristofferson, A. B. Successiveness discrimination as a two-state, quantal process. *Science* **158**, 1337–1339 (1967).
6. Samaha, J. & Romei, V. Alpha-band frequency and temporal windows in perception: a review and living meta-analysis of 27 experiments (and counting). *J. Cogn. Neurosci.* **36**, 640–654 (2024).
7. Samaha, J. & Romei, V. Alpha-band Brain Dynamics and Temporal Processing: An Introduction to the Special Focus. *J Cogn Neurosci* 1–5. https://doi.org/10.1162/jocn_a_02105 (2024).
8. Frisoni, M., Tarasi, L., Borgomaneri, S. & Romei, V. The relationship between individual alpha frequency and time perception: Testing the internal clock versus the sampling rate hypothesis. *Cortex* **192**, 183–195 (2025).
9. Samaha, J. & Postle, B. R. The speed of alpha-band oscillations predicts the temporal resolution of visual perception. *Curr. Biol.* **25**, 2985–2990 (2015).
10. Deodato, M. & Melcher, D. Correlations between Visual Temporal Resolution and Individual Alpha Peak Frequency: Evidence that Internal and Measurement Noise Drive Null Findings. *J Cogn Neurosci* 1–12. https://doi.org/10.1162/jocn_a_01993 (2023).
11. Cecere, R., Rees, G. & Romei, V. Individual differences in alpha frequency drive crossmodal illusory perception. *Curr. Biol.* **25**, 231–235 (2015).
12. Cooke, J., Poch, C., Gillmeister, H., Costantini, M. & Romei, V. Oscillatory properties of functional connections between sensory areas mediate cross-modal illusory perception. *J. Neurosci.* **39**, 5711–5718 (2019).
13. Tarasi, L. & Romei, V. Individual alpha frequency contributes to the precision of human visual processing. *J. Cogn. Neurosci.* 1–11. https://doi.org/10.1162/jocn_a_02026 (2023).
14. Venskus, A. et al. Temporal binding window and sense of agency are related processes modifiable via occipital tACS. *PLoS ONE* **16**, e0256987 (2021).
15. Zhang, Y., Zhang, Y., Cai, P., Luo, H. & Fang, F. The causal role of α-oscillations in feature binding. *Proc. Natl. Acad. Sci. USA* **116**, 17023–17028 (2019).
16. Sharp, P., Gutteling, T., Melcher, D. & Hickey, C. Spatial attention tunes temporal processing in early visual cortex by speeding and slowing alpha oscillations. *J. Neurosci.* **42**, 7824–7832 (2022).
17. Wutz, A., Melcher, D. & Samaha, J. Frequency modulation of neural oscillations according to visual task demands. *Proc. Natl. Acad. Sci. USA* **115**, 1346–1351 (2018).
18. Buergers, S. & Noppeney, U. The role of alpha oscillations in temporal binding within and across the senses. *Nat. Hum. Behav.* **6**, 732–742 (2022).
19. Di Gregorio, F. et al. Tuning alpha rhythms to shape conscious visual perception. *Curr. Biol.* https://doi.org/10.1016/j.cub.2022.01.003 (2022).
20. Dugué, L., Marque, P. & VanRullen, R. The phase of ongoing oscillations mediates the causal relation between brain excitation and visual perception. *J. Neurosci.* **31**, 11889–11893 (2011).
21. Mathewson, K. E., Gratton, G., Fabiani, M., Beck, D. M. & Ro, T. To see or not to see: prestimulus alpha phase predicts visual awareness. *J. Neurosci.* **29**, 2725–2732 (2009).
22. Busch, N. A., Dubois, J. & VanRullen, R. The phase of ongoing EEG oscillations predicts visual perception. *J. Neurosci.* **29**, 7869–7876 (2009).
23. Ratcliff, R., Smith, P. L., Brown, S. D. & McKoon, G. Diffusion decision model: current issues and history. *Trends Cogn. Sci.* **20**, 260–281 (2016).
24. Tarasi, L., di Pellegrino, G. & Romei, V. Are you an empiricist or a believer? Neural signatures of predictive strategies in humans. *Prog. Neurobiol.* **219**, 102367 (2022).
25. Tarasi, L. et al. Oscillatory signatures of monitoring and anticipatory strategies for probabilistic vs deterministic cues. *Imaging Neurosci.* **3**, imag_a_00496 (2025).
26. Cohen, M. X. & Cavanagh, J. F. Single-trial regression elucidates the role of prefrontal theta oscillations in response conflict. *Front Psychol.* **2**, 30 (2011).
27. Cohen, M. X. *Analyzing Neural Time Series Data: Theory and Practice*. https://doi.org/10.7551/mitpress/9609.001.0001 (2014).
28. Samaha, J., Iemi, L. & Postle, B. R. Prestimulus alpha-band power biases visual discrimination confidence, but not accuracy. *Conscious Cogn.* **54**, 47–55 (2017).
29. Di Luzio, P., Tarasi, L., Silvanto, J., Avenanti, A. & Romei, V. Human perceptual and metacognitive decision-making rely on distinct brain networks. *PLoS Biol.* **20**, e3001750 (2022).
30. Di Luzio, P. et al. Targeted neuromodulation of perceptual decision-making networks causally dissociates sensory and metacognitive performance. Preprint at https://doi.org/10.1101/2025.05.15.653831 (2025).
31. Ippolito, G. et al. The role of alpha oscillations among the main neuropsychiatric disorders in the adult and developing human brain: evidence from the last 10 years of research. *Biomedicines* **10**, 3189 (2022).
32. Alamia, A. & VanRullen, R. Alpha oscillations and traveling waves: signatures of predictive coding?. *PLoS Biol.* **17**, e3000487 (2019).
33. Clayton, M. S., Yeung, N. & Cohen Kadosh, R. The many characters of visual alpha oscillations. *Eur. J. Neurosci.* **48**, 2498–2508 (2018).
34. Ronconi, L., Oosterhof, N. N., Bonmassar, C. & Melcher, D. Multiple oscillatory rhythms determine the temporal organization of perception. *Proc. Natl. Acad. Sci.* **114**, 13435–13440 (2017).
35. Tarasi, L., Alamia, A. & Romei, V. Backward alpha band oscillations shape perceptual bias under probabilistic cues. *Commun. Biol.* **9**, 280 (2026).
36. Tarasi, L., Alamia, A. & Romei, V. Perceptual bias in motion discrimination is related to asymmetric interhemispheric alpha traveling waves. *Adv. Sci.* **12**, e14623 (2025).

37. Noguchi, Y. Individual differences in beta frequency correlate with the audio–visual fusion illusion. *Psychophysiology* **59**, e14041 (2022).
38. Migliorati, D. et al. Individual alpha frequency predicts perceived visuotactile simultaneity. *J. Cogn. Neurosci.* **32**, 1–11 (2020).
39. Ronconi, L., Busch, N. A. & Melcher, D. Alpha-band sensory entrainment alters the duration of temporal windows in visual perception. *Sci. Rep.* **8**, 11810 (2018).
40. Trajkovic, J. et al. Resting state alpha oscillatory activity is a valid and reliable marker of schizotypy. *Sci. Rep.* **11**, 10379 (2021).
41. Ramsay, I. S., Lynn, P., Schermitzler, B. & Sponheim, S. Individual alpha peak frequency is slower in schizophrenia and related to deficits in visual perception and cognition. *Sci. Rep.* **11**, 17852 (2021).
42. Nelli, S., Itthipuripat, S., Srinivasan, R. & Serences, J. T. Fluctuations in instantaneous frequency predict alpha amplitude during visual perception. *Nat. Commun.* **8**, 2071 (2017).
43. Ai, L. & Ro, T. The phase of prestimulus alpha oscillations affects tactile perception. *J. Neurophysiol.* **111**, 1300–1307 (2014).
44. Minami, S., Oishi, H., Takemura, H. & Amano, K. Inter-individual differences in occipital alpha oscillations correlate with white matter tissue properties of the optic radiation. *eNeuro* **7**, ENEURO.0224–19.2020 (2020).
45. Smit, C. M., Wright, M. J., Hansell, N. K., Geffen, G. M. & Martin, N. G. Genetic variation of individual alpha frequency (IAF) and alpha power in a large adolescent twin sample. *Int. J. Psychophysiol.* **61**, 235–243 (2006).
46. Klimesch, W. EEG alpha and theta oscillations reflect cognitive and memory performance: a review and analysis. *Brain Res. Rev.* **29**, 169–195 (1999).
47. Karvat, G. & Landau, A. N. A role for bottom–up alpha oscillations in temporal integration. *J. Cogn. Neurosci.* **36**, 632–639 (2024).
48. Haegens, S., Cousijn, H., Wallis, G., Harrison, P. J. & Nobre, A. C. Inter- and intra-individual variability in alpha peak frequency. *NeuroImage* **92**, 46–55 (2014).
49. Trajkovic, J., Di Gregorio, F., Thut, G. & Romei, V. Transcranial magnetic stimulation effects support an oscillatory model of ERP genesis. *Curr. Biol.* **34**, 1048–1058.e4 (2024).
50. Bertaccini, R. et al. Rhythmic TMS as a feasible tool to uncover the oscillatory signatures of audiovisual integration. *Biomedicines* **11**, 1746 (2023).
51. Santoni, A. et al. Bifocal alpha-band tACS modulates temporal sampling in visual perception. *NeuroImage* **320**, 121474 (2025).
52. Canolty, R. T. & Knight, R. T. The functional role of cross-frequency coupling. *Trends Cogn. Sci.* **14**, 506–515 (2010).
53. Tarasi, L., Romanazzi, D., Pasini, A. & Romei, V. Delusion-like thinking is associated with lower individual alpha peak frequency. *Schizophrenia* **11**, 76 (2025).
54. Tarasi, L. et al. Predictive waves in the autism-schizophrenia continuum: a novel biobehavioral model. *Neurosci. Biobehav. Rev.* **132**, 1–22 (2022).
55. Tarasi, L., Martelli, M. E., Bortoletto, M., di Pellegrino, G. & Romei, V. Neural signatures of predictive strategies track individuals along the autism-schizophrenia continuum. *Schizophr. Bull.* **49**, 1294–1304 (2023).
56. Tarasi, L., Borgomaneri, S. & Romei, V. Antivax attitude in the general population along the autism-schizophrenia continuum and the impact of socio-demographic factors. *Front. Psychol.* **14**, 1059676 (2023).
57. Tarasi, L. et al. Preparing to act follows Bayesian inference rules. *iScience* **28**, 112645 (2025).
58. Sterzer, P. et al. The predictive coding account of psychosis. *Biol. Psychiatry* **84**, 634–643 (2018).
59. Tarasi, L. & Romei, V. Predictive inference alterations in psychosis proneness are context-dependent. Preprint at https://doi.org/10.1101/2025.05.17.654666 (2025).
60. Benwell, C. S. Y. et al. Prestimulus EEG power predicts conscious awareness but not objective visual performance. *eNeuro* **4**, ENEURO.0182-17.2017 (2017).
61. Ruzzoli, M., Torralba, M., Morís Fernández, L. & Soto-Faraco, S. The relevance of alpha phase in human perception. *Cortex* **120**, 249–268 (2019).
62. Tseng, C.-H., Chen, J.-H. & Hsu, S.-M. The effect of the peristimulus α phase on visual perception through real-time phase-locked stimulus presentation. *eNeuro* **10**, ENEURO.0128-23.2023 (2023).
63. Fakche, C., VanRullen, R., Marque, P. & Dugué, L. α Phase-Amplitude Tradeoffs Predict Visual Perception. *eNeuro* **9**, ENEURO.0244-21.2022 (2022).
64. Deodato, M. & Melcher, D. Aperiodic EEG Predicts Variability of Visual Temporal Processing. *J. Neurosci.* **44**, e2308232024 (2024).
65. Popov, T., Gips, B., Weisz, N. & Jensen, O. Brain areas associated with visual spatial attention display topographic organization during auditory spatial attention. *Cereb. Cortex* **33**, 3478–3489 (2023).
66. Green, D. M. & Swets, J. A. *Signal Detection Theory and Psychophysics* (John Wiley & Sons, New York, 1966).
67. Levitt, H. Transformed up–down methods in psychoacoustics. *J. Acoust. Soc. Am.* **49**, 467–477 (1971).
68. Delorme, A. & Makeig, S. EEGLAB: an open source toolbox for analysis of single-trial EEG dynamics including independent component analysis. *J. Neurosci. Methods* **134**, 9–21 (2004).
69. Cohen, M. X. Fluctuations in oscillation frequency control spike timing and coordinate neural networks. *J. Neurosci.* **34**, 8988–8998 (2014).
70. Samaha, J. & Cohen, M. X. Power spectrum slope confounds estimation of instantaneous oscillatory frequency. *Neuroimage* **250**, 118929 (2022).
71. Rassi, E., Lin, W. M., Zhang, Y., Emmerzaal, J. & Haegens, S. β Band Rhythms Influence Reaction Times. *eNeuro* **10**, ENEURO.0473-22.2023 (2023).
72. Corcoran, A. W., Alday, P. M., Schlesewsky, M. & Bornkessel-Schlesewsky, I. Toward a reliable, automated method of individual alpha frequency (IAF) quantification. *Psychophysiology* **55**, e13064 (2018).
73. Schoffelen, J.-M., Pesci, U. G. & Noppeney, U. Alpha oscillations and temporal binding windows in perception—a critical review and best practice guidelines. *J. Cogn. Neurosci.* **36**, 655–690 (2024).
74. Macmillan, N. A. & Kaplan, H. L. Detection theory analysis of group data: Estimating sensitivity from average hit and false-alarm rates. *Psychol. Bull.* **98**, 185–199 (1985).
75. Wiecki, T., Sofer, I. & Frank, M. HDDM: Hierarchical Bayesian estimation of the drift-diffusion model in Python. *Front. Neuroinform.* **7**, 14 (2013).
76. Matzke, D. & Wagenmakers, E.-J. Psychological interpretation of the ex-Gaussian and shifted Wald parameters: a diffusion model analysis. *Psychon. Bull. Rev.* **16**, 798–817 (2009).
77. Hussain, S. J. et al. Sensorimotor oscillatory phase-power interaction gates resting human corticospinal output. *Cereb. Cortex* **29**, 3766–3777 (2019).
78. Zrenner, C., Desideri, D., Belardinelli, P. & Ziemann, U. Real-time EEG-defined excitability states determine efficacy of TMS-induced plasticity in human motor cortex. *Brain Stimul.* **11**, 374–389 (2018).
79. Michail, G., Toran Jenner, L. & Keil, J. Prestimulus alpha power but not phase influences visual discrimination of long-duration visual stimuli. *Eur. J. Neurosci.* **55**, 3141–3153 (2022).
80. Berens, P. CircStat: a MATLAB toolbox for circular statistics. *J. Stat. Softw.* **31**, 1–21 (2009).
81. Arnal, L. H. & Giraud, A.-L. Cortical oscillations and sensory predictions. *Trends Cogn. Sci.* **16**, 390–398 (2012).
82. Samaha, J., Bauer, P., Cimaroli, S. & Postle, B. R. Top-down control of the phase of alpha-band oscillations as a mechanism for temporal prediction. *Proc. Natl. Acad. Sci.* **112**, 8439–8444 (2015).

83. VanRullen, R. How to evaluate phase differences between trial groups in ongoing electrophysiological signals. *Front. Neurosci.* **10**, 426 (2016).
84. Rideaux, R., West, R. K., Rangelov, D. & Mattingley, J. B. Distinct early and late neural mechanisms regulate feature-specific sensory adaptation in the human visual system. *Proc. Natl. Acad. Sci.* **120**, e2216192120 (2023).

Acknowledgements

This study was funded by the European Union—NextGenerationEU, in the framework of the NRRP - M4C2 - I1.1 - P2022XAKXL_003. The views and opinions expressed are solely those of the authors and do not necessarily reflect those of the European Union, nor can the European Union be held responsible for them.

Author contributions

Vincenzo Romei: Conceptualisation; Funding acquisition; Project administration; Supervision; Writing—Original draft; Writing—Review and editing. Luca Tarasi: Conceptualisation; Data collection; Formal Analysis; Writing—Original draft; Writing—Review and editing.

Competing interests

The authors declare no competing interests.

Additional information

Supplementary information The online version contains supplementary material available at https://doi.org/10.1038/s41467-026-70124-9.

Correspondence and requests for materials should be addressed to Vincenzo Romei or Luca Tarasi.

Peer review information *Nature Communications* thanks David Melcher, Mehdi Senoussi, Nathan Weisz, Tim Rohe and the other, anonymous, reviewer(s) for their contribution to the peer review of this work. A peer review file is available.